NASA TN D-1749

TECHNICAL NOTE

D-1749

ENERGETIC PARTICLES IN THE INNER VAN ALLEN BELT

Wilmot N. Hess

Goddard Space Flight Center
Greenbelt, Maryland

NATIONAL AERONAUTICS AND SPACE ADMINISTRATION
WASHINGTON

July 1963

ENERGETIC PARTICLES IN THE INNER VAN ALLEN BELT

by
Wilmot N. Hess
Goddard Space Flight Center

SUMMARY

A survey is given of the high-energy particle populations in the inner radiation belt. The experiments which have given information about particles are discussed and the best experimental information about particle fluxes and spectra is presented. Calculations are given which indicate what particle sources and loss processes are most important. The role of neutrons in making the inner belt is considered in detail and the need for particle acceleration and/or other sources of particles is shown.

CONTENTS

ENERGETIC PARTICLES IN THE INNER VAN ALLEN BELT

by
Wilmot N. Hess
Goddard Space Flight Center

INTRODUCTION

The satellite Explorer I (1958 α) launched with a Geiger-Müller counter on board discovered a region of high count rate starting at an altitude of about 1000 km. This was unexpected—in fact, it was suggested that the counter might have malfunctioned. But results from Explorer III (1958 γ) demonstrated that the effect was real. Van Allen, who had conducted both experiments (Reference 1), realized very soon that the measured high count rates were due to charged particles trapped in the earth's magnetic field (Reference 2). Störmer had worked extensively on this general subject (Reference 3) and even calculated orbits of trapped particles (Reference 4) years earlier, but the actual existence of trapped particles had not been suggested in this work. Ideas about the existence of a terrestrial ring current had also essentially included the idea of trapped particles (Reference 5).

At the same time that these experiments in space were going on, experiments with trapped particles were going on in various laboratories. Project Sherwood is an attempt by the Atomic Energy Commission to make a controlled thermonuclear reaction on a small scale (Reference 6) by confining charged particles in a magnetic field. Christofilos, who was working on Project Sherwood, extrapolated the laboratory idea to earth scale and suggested the possibility of trapping a large number of charged particles in the earth's magnetic field by using a nuclear explosion to inject the particles. This idea was carried out in the Argus Experiment (Reference 7) and demonstrated experimentally that charged particles could really be trapped in the earth's field. It had even been suggested in planning the Argus Experiment that a natural radiation belt, populated by the decay of neutrons escaping from the earth's atmosphere might exist; but this idea did not get wide distribution.

Results obtained from Sputnik III (1958 $\delta 2$) in May 1958 confirmed the existence of the trapped radiation with measurements up to 1800 km (References 8 and 9).

Explorer IV (1958 ϵ) was launched in July 1958 with instrumentation to study the natural radiation belt (Reference 10) and to study the artificial belt produced by Argus (Reference 11). A map of the radiation intensities up to an altitude of 2200 km and a range spectrum of the charged particles were obtained by Explorer IV.

Pioneer III (1958 θ1) in December 1958 (Reference 12) and Pioneer IV (1959 ν) in March 1959 (Reference 13) made isolated passes more or less radially outwards through the inner belt. More recently, Injun (1961 o2) and Explorer VII (1959 ι 1) and several Discoverer satellites have given information about the inner belt. These, with various rocket shots, complete the list of experiments performed.

In this report, an attempt is made to survey the experiments that have given information about the inner belt and also the calculations that have been made dealing with energetic particles in this area. One subject that will receive special attention is neutrons in space and neutron decay, because it is well established that neutrons play a major role in the production of protons and also probably of electrons in the inner belt.

MOTION OF PARTICLES IN A DIPOLE FIELD

The general problem of charged particle motion in a dipole field is complicated (Reference 3). Fortunately, for radiation belt particles, an approximation can be used which simplifies the situation considerably. Alfvén (Reference 14) introduced the idea of the *guiding center* of a particle. The particle motion in this case is described in terms of: (1) a rapid gyration about a *guiding center* with a cyclotron period τ_c and radius of gyration R_c, and (2) motion of this guiding center along a magnetic line of force. The motion along the line is periodic too. The particle is reflected by the converging magnetic field near the earth and bounces back and forth in the exosphere with a bounce period τ_B. There is another motion (Reference 15), a slow drift in longitude around the earth with a period of revolution of τ_R. Particles at 2000 km altitude near the equator will have the characteristics listed in Table 1. Because the three periods are so different, the particle motion is separable into these three components. If the cyclotron radius of the particle R_c becomes comparable to the diameter of the earth, the motion is not separable; however, even for 1 Bev protons this condition does not occur.

Table 1

Characteristics of Particles at 2000 km Altitude Near the Equator.

Particle	R_c (cm)	τ_c (sec)	τ_B (sec)	τ_R (min)
50 kev Electron	5×10^3	2.5×10^{-6}	0.25	690
1 Mev Electron	3.2×10^4	7×10^{-6}	0.10	53
1 Mev Proton	1×10^6	4×10^{-3}	2.2	32
10 Mev Proton	3×10^6	42×10^{-3}	0.65	3.2
500 Mev Proton	2.5×10^7	6×10^{-3}	0.11	0.084

We can understand the particle's bouncing motion in the following way (Reference 16). A static magnetic field does no work on a particle; therefore, the flux linking the orbit of a particle rotating about a field line is constant. If $d\Phi/dt = 0$, the particle's energy would change. Thus,

$$\Phi = B\pi R_c^2 = \text{constant}, \tag{1}$$

and we can write for the particle's perpendicular energy

$$E_\perp = \frac{mV_\perp^2}{2} = \frac{m\omega^2 R_c^2}{2} = \frac{mR^2}{2}\left(\frac{eB}{mc}\right)^2 = \frac{e^2 B^2 R_c^2}{2mc^2} \quad . \tag{2}$$

Substituting this into Equation 1, we get

$$\Phi = \text{constant} = \frac{2\pi mc^2 E_\perp}{e^2 B} \; ; \tag{3}$$

therefore,

$$\frac{E_\perp}{B} = \text{constant} = \mu \; . \tag{4}$$

The constant μ is the magnetic moment of the particle's motion around the field line.

From Equation 4 we see that

$$\frac{\sin^2 \alpha}{B} = \text{constant.} \tag{5}$$

The particle will move into a region of increasing B until $\sin \alpha = 1$ when it must turn around. It then moves out of the high field region and repeats the process at the other end of the field line for the same value of B. The angle α is the particle's pitch angle.

The drift in longitude of a charged particle results from a force on the particle perpendicular to the field lines and lying in the plane through the center of the earth containing the earth's axis. The magnitude and direction of this drift velocity can be obtained from the cyclotron equation

$$\mathbf{R} = \frac{mc}{eB^2}(\mathbf{v} \times \mathbf{B}) = \frac{c}{eB^2}(\mathbf{p} \times \mathbf{B}) \; . \tag{6}$$

If a force $f_\perp$ acts perpendicular to B for a time Δt, there is a change of momentum of

$$\Delta p = f_\perp \Delta t \; ; \tag{7}$$

this results in a displacement of the guiding center of the particle of

$$\Delta \mathbf{R} = \frac{c}{eB^2}(\Delta \mathbf{p} \times \mathbf{B}). \tag{8}$$

Differentiating Equation 8 with respect to time gives

$$v_D = \frac{dR}{dt} = \frac{c}{eB^2}\left(f_\perp \times B\right) . \tag{9}$$

This drift velocity is perpendicular to both $f_\perp$ and B; therefore, if $f_\perp$ lies in the plane through the center of the earth containing the earth's axis, the drift velocity will be azimuthal—a drift in longitude.

One force that produces a drift is due to the gradient of the earth's magnetic field:

$$f_\perp = \mu v B = \frac{3\mu B}{R} . \tag{10}$$

A second force that produces a drift is the centrifugal force on a particle due to the curvature of field lines:

$$f_\perp = \frac{m v_{11}^2}{R_l} . \tag{11}$$

Combining these gives a drift velocity

$$\nu_D = \frac{1}{\omega_c R_c}\left(\nu_\parallel^2 + \frac{1}{2}\nu_\perp^2\right) , \tag{12}$$

where ω_c and R_c are the cyclotron frequency and radius, respectively.

There is also a possibility of radial drift of particles due to line exchange (Reference 17) or other effects (Reference 18), but these drifts do not seem to be important for high-energy trapped particles as was demonstrated by the spatial stability of the Argus electrons.

ADIABATIC INVARIANTS

Associated with the motion of particles in a dipole field are three constants. They are actually only adiabatic constants—in other words they are constant unless magnetic fields change rapidly. We have shown the magnetic moment μ to be a constant of the motion, but it is not constant if fields change in times short compared to τ_c or in distances short compared to R_c .

The second adiabatic (Reference 19) invariant I is called the integral invariant,

$$I = \frac{1}{\nu}\int_{m_1}^{m_2} v_{11}\, dl , \tag{13}$$

where the integral is taken along a field line between the two mirror points. This quantity is related to the Hamilton action integral and is violated if changes occur in times short compared to τ_B.

The third invariant is the flux invariant (Reference 20). When this invariant holds, the magnetic flux linked by the particle's orbit is constant. This is violated if field changes occur in times short compared to τ_R.

We can understand the motion of a particle in the earth's field rather well by considering only the constancy of μ and I. From μ we know that the particle mirrors at a particular value of B. From I we can determine which field line the particle will travel as it drifts around the earth. The combination of these two defines a surface around the earth, resembling the surface of a pitted olive, on which the particle will travel.

SOURCES OF THE BELT PARTICLES

Cosmic Rays

A flux of about 2 particles/cm^2-sec of galactic cosmic rays reaches the earth regularly. One possibility about the radiation belts is that they represent quasi-trapped particles (Reference 21), that is, they consist of particles on certain special Störmer orbits that can stay near the earth for a long time and then finally move out of the earth's field and escape. Estimates of the intensity of the radiation belt that would be produced this way show this to be a small effect. A flux increase by a factor of 10^4 or more over the galactic cosmic rays would be needed to produce the radiation belt fluxes. The increase obtained by this quasi-trapping is nowhere near 10^4.

Another possibility is that cosmic rays might produce trapped particles by interacting with the very thin atmosphere at very high altitude. We can estimate the importance of this source. If we take an atmospheric density of 10^5 atoms/cm^3 of oxygen and a cross section for producing high-energy charged particles of 0.2×10^{-24} cm^2, we get a source strength S of

$$S = \left(\frac{2 \text{ protons}}{\text{cm}^2\text{-sec}}\right)\left(\frac{10^5 \text{ atoms}}{\text{cm}^3}\right)\left(\frac{0.2 \times 10^{-24}\,\text{cm}^2}{\text{atom}}\right)$$

$$= \frac{4 \times 10^{-20} \text{ protons}}{\text{cm}^3\text{-sec}} .$$

This also is negligible when compared to other source strengths.

Still another possible source of the belt particles is splash albedo protons produced by interactions of the high-energy cosmic rays with the atmosphere. We know that the particles must return to roughly their birth altitude or even lower in order to mirror at the other end of their line of force. They must therefore encounter a rather thick atmosphere and be rapidly lost, so this source contributes little, if anything.

Mu Mesons

High-energy collisions involving cosmic rays produce π mesons. These decay in about 10^{-8} sec to μ mesons which in turn decay in 2×10^{-6} sec to electrons having energies up to 50 Mev. If the decay

occurs at a high enough altitude, the electron can be trapped. A μ meson, to travel 1000 km, must live 0.003 sec. Even if it lives 5 half-lives or 10^{-5} sec, it must have a relativistic time dilation factor of $\gamma = .003/10^{-5} = 300$ in order to travel this distance. Thus it must have an energy on the order of 300×106 Mev = 30 Bev. There are very few 30 Bev μ mesons made traveling upwards out of the atmosphere, and this source can also be neglected.

Solar Wind

There are about 10 protons/cm^3 in the kev energy range striking the magnetosphere (Reference 22); this is a large flux of particles. If they could be brought into the magnetic field of the earth, they could be an important source. There are several possibilities here. Particles may be injected at the field nulls near the poles (Reference 23). Field convection processes may bring them into the field (Reference 24); Taylor instabilities may also help them get in. All of these are possible but none of them are understood well enough to be evaluated. It would appear that some processes of this sort may produce low energy particles in the outer belt, but it seems difficult to see how particles can be brought in through the outer belt to the inner belt efficiently. For want of any specific information about these processes we will not consider them further.

Neutrons

Neutrons are made by cosmic ray protons colliding with oxygen and nitrogen nuclei in the atmosphere. Several neutrons are made in the nuclear cascade in the atmosphere. A 5 Bev cosmic ray proton will produce about 7 neutrons in the atmosphere. About 25 percent of all neutrons produced this way diffuse out into space; this leakage flux of neutrons out of the atmosphere is about 0.5 neutrons/cm^2-sec at the equator and about 5 neutrons/cm^2-sec at the pole. The neutron flux in space close to the earth at low latitudes has been measured (Reference 25) to be about 1.0 neutrons/cm^2-sec; this is in reasonable agreement with the calculated fluxes. Few neutrons reach the earth from the sun or more distant space because the free neutron is radioactive with a mean life of only 1000 sec. It decays by the reaction

$$n \rightarrow p + e + \bar{\nu} .$$

The antineutrino $\bar{\nu}$ does not interest us here, but the proton and electron are both important in forming the radiation belt.

We need to know how many neutrons of what energies decay at different places in space to produce protons and electrons. First, we must know the neutron energy spectrum $\Phi_n(E,R,\lambda)$ in space at all radii R and latitudes λ. This has been calculated (Reference 26) from a knowledge of the neutron energy spectrum inside the atmosphere (Reference 27) and is shown in Figure 1. The flux decreases as a function of height above the earth. This is especially true for low-energy neutrons. Neutrons of less than 2/3 ev are trapped by the earth's gravitational field so that they essentially all decay in space

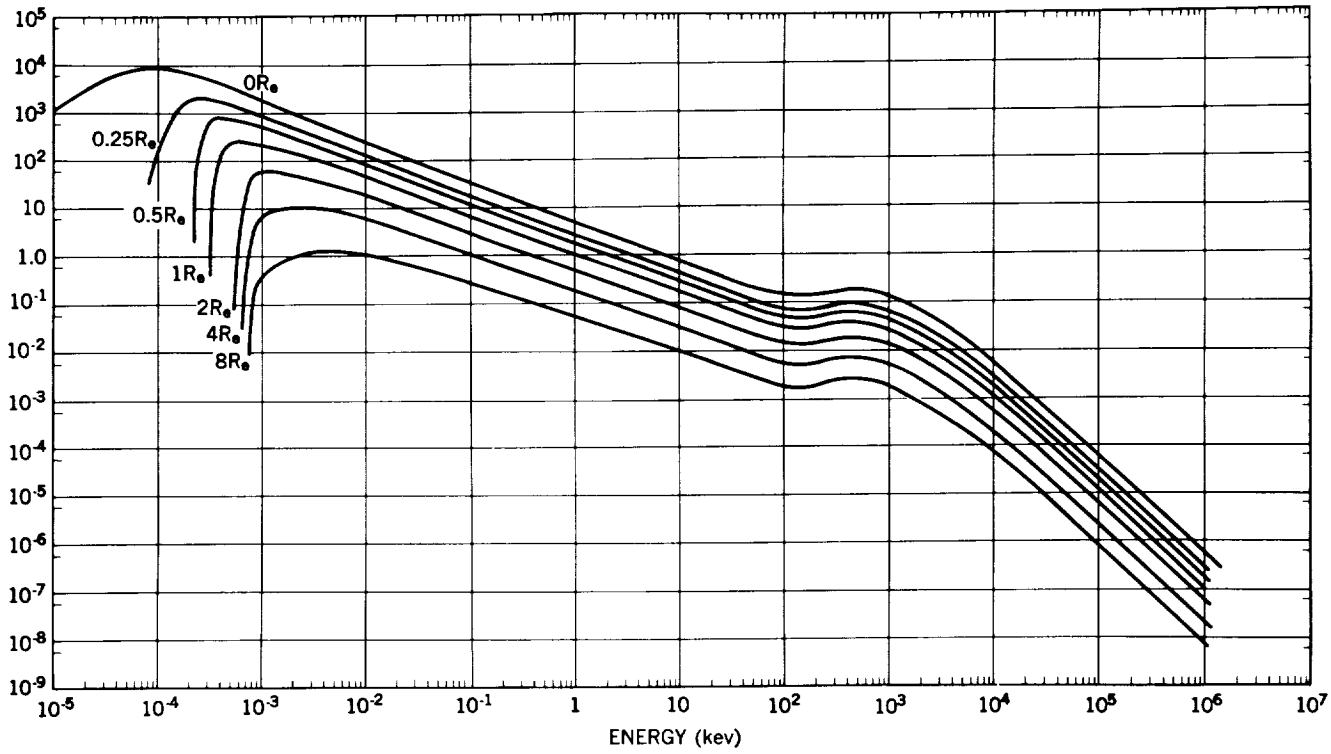

Figure 1—Albedo neutron energy spectra in space at different distances above the geomagnetic equator on December 5, 1959. The zero R_e curve is for the top of the atmosphere, roughly 100 km. Reproduced with permission from References 26 and 27.

near the earth, while only about 1 percent of neutrons of 1 Mev energy decay near the earth. The density of neutrons decaying is given by

$$\frac{dn}{dV}(E,R,\lambda) = \frac{1}{\gamma v(E)\tau_n}\Phi_n(E,R,\lambda) , \qquad (14)$$

where v is the neutron velocity and τ_n the neutron mean life.

The electrons made by the neutron decay will have the β decay spectrum shown in Figure 2. The electron's energy will be essentially unchanged by the neutron's kinetic energy. To demonstrate this, consider a 10 Mev

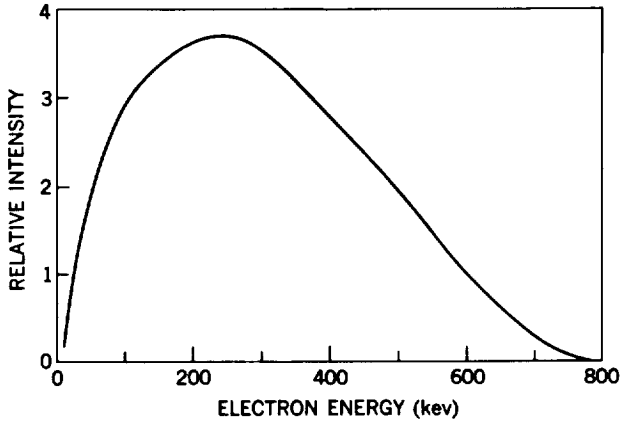

Figure 2—The electron-energy spectrum from neutron β decay. To obtain electron flux multiply the intensity by the electron velocity.

neutron, which has a velocity of about 4×10^9 cm/sec. When an electron of about 30 kev energy is produced by the neutron decay it has a velocity of about 2×10^{10} cm/sec. When the neutron's velocity is compounded with this velocity relativistically it changes by, at most, 10 percent. Almost all neutrons have energies less than 10 Mev, so the effect of the neutron's motion in changing the electron's energy can be neglected. Therefore, to determine the total electron source strength S_e for the radiation belt due to neutron decay, we simply add up all neutron decay events:

$$S_e\ (R,\lambda) = \int \frac{dn}{dV}\,(E,R,\lambda)\ dE = \int \frac{1}{\gamma v \tau_n}\,\Phi(E,R,\lambda)\ dE\ . \tag{15}$$

This electron source strength S_e is shown in Figure 3. We see there are from 10^{-13} to 10^{-12} electrons/cm^3-sec made by this source in space near the earth.

The situation is different when we consider the protons made by neutron decay. The kinetic energy of the proton is very nearly the kinetic energy of its parent neutron. The electron kinetic energy is supplied by the mass difference of the neutron and proton. The recoil energy given the proton by the electron is only about 100 ev; so, if we consider protons above about 10 kev, we can accurately take the proton's energy and direction of motion to be that of the parent neutron. Because of this the decay density energy spectrum shown in Figure 4 is also the proton source energy spectrum $S_p\ (E,R,\lambda)$ from about 10 kev up,

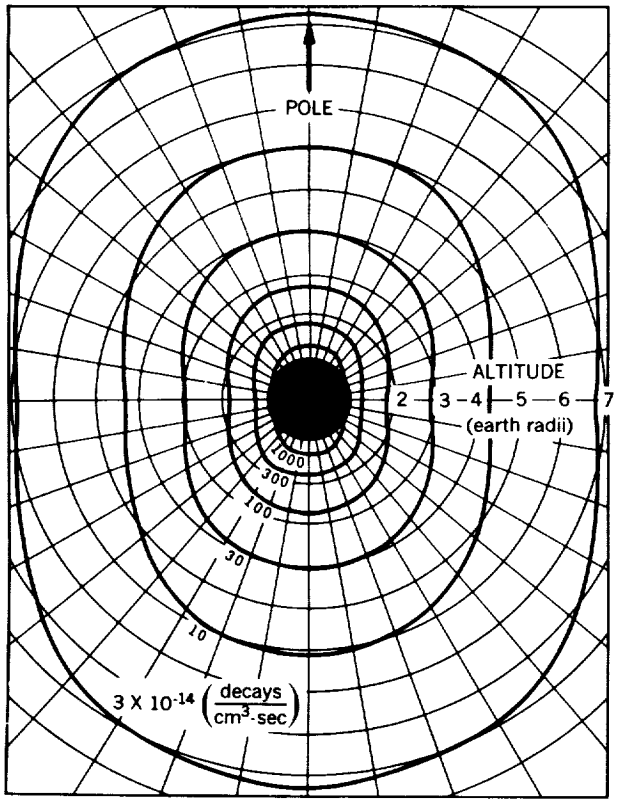

Figure 3—Values of the neutron decay density dn/dV summed over neutron energy at different attitudes and magnetic latitudes. Reproduced with permission from Reference 26.

$$S_p\ (E,R,\lambda) = \frac{dn}{dV}\,(E,R,\lambda)\ . \tag{16}$$

There are about 6×10^{-15} protons/cm^3-sec of $E > 10$ Mev produced in space near the earth. The proton source near the earth at the equator has been evaluated from Figure 1 to be

$$S_p\ (E,R_e,0) = \frac{0.8\,E^{-2.0}}{\gamma v \tau_n}\ . \tag{17}$$

We have a quantitative picture of the neutron-decay proton and electron sources. These are an important source of the radiation belts.

LOSS PROCESSES

Protons

There are at least three ways in which protons are lost from the radiation belt. In the inner belt, high-energy protons are removed most rapidly by slowing down until they reach about 100 kev. The amounts of oxygen R that must be traversed to stop protons of various energies are listed in Table 2.

Table 2

Ranges of Protons in Oxygen.

Energy (Mev)	Range (gm/cm^2)
0.1	6×10^{-5}
1	0.003
10	0.14
100	8.6

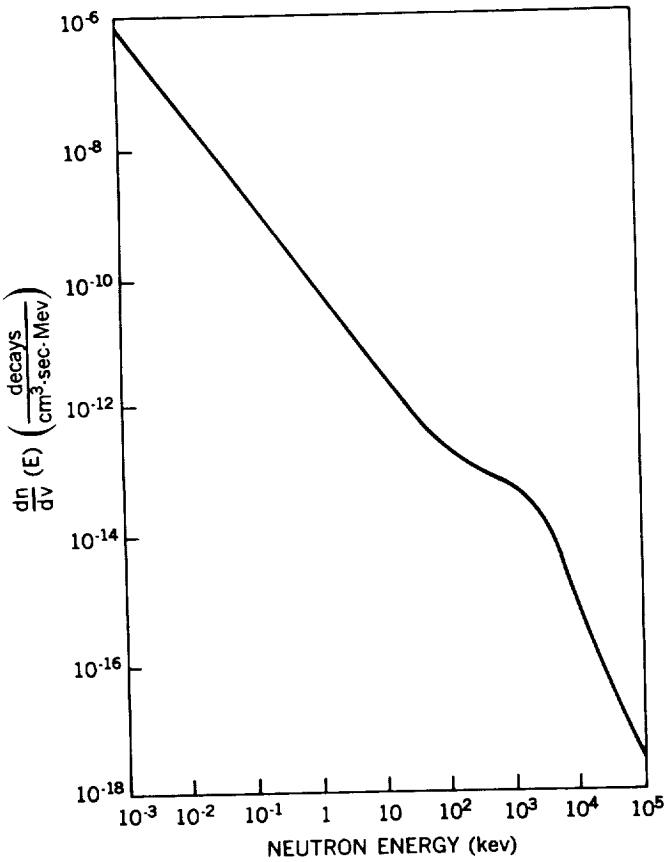

Figure 4—The neutron decay energy spectrum dn/dV(E) at 1500 km on the equator.

Below 100 kev, the protons are more rapidly lost by charge exchange (Reference 28) with slow protons by the reaction

$$\underline{p} + H \rightarrow p + \underline{H} ,$$

where the bar refers to the fast particle. At 50 kev, the cross section for charge exchange (Reference 29) is $\sigma_{cH} = 2 \times 10^{-16}\ \text{cm}^2$, and the charge exchange lifetime τ_{cH} is given by

$$\tau_{cH} = \frac{1}{\sigma_{cH}\, n(H)\, \nu} = \frac{1}{\left(2 \times 10^{-16}\ \text{cm}^2\right)\left(10^4\ \frac{\text{atoms}}{\text{cm}^3}\right)\left(3 \times 10^8\ \frac{\text{cm}}{\text{sec}}\right)} = 1600\ \text{sec} , \tag{18}$$

where n(H) is the atomic density of hydrogen, taken here to be 10^4 atoms/cm^3. This time is less than the slowing down time above approximately 1000 km altitude, so the charge exchange process will dominate here.

In the outer belt, protons are lost rapidly by some additional process. Probably this involves the breakdown of the magnetic moment invariant. Various possibilities along this line are considered later.

Electrons

Different processes are responsible for the loss of electrons than for protons. Because electrons are lighter, they scatter more easily and are lost in the inner belt principally by coulomb scattering into the loss cone rather than by slowing down. This can be seen by comparing R, the range of the particle, and D, the amount of material necessary to scatter out. The range of a 1 Mev electron, from Feather's rule, is

$$R = 0.54\,E - 0.13 = 0.41\ \frac{gm}{cm^2} \quad . \tag{19}$$

The value of D can be obtained by using the scattering formula (Reference 30)

$$\theta^2 = \frac{7000\,D}{E^2} \quad , \tag{20}$$

where θ^2 is the mean angle of scattering, D is the path length of air (at S.T.P.) traversed in cm, and E is the particle energy in kev. Taking $\theta = 0.5$ rad as the necessary scattering angle to lose the particle, we find

$$D = 0.04\ \frac{gm}{cm^2} \quad .$$

This shows the electron will be scattered out of the inner belt before it slows down.

HIGH-ENERGY PROTONS

Experiments on the Energy Spectrum

The first experiment performed in the radiation belt that unambiguously identified the particles which were counted involved flying a stack of nuclear emulsions on the Atlas rocket (Reference 31). The emulsion stack was recovered and developed and the nuclear tracks were read. The range and ionization of the particles were measured, the particles identified and their energies determined.

Protons of $E > 75$ Mev and electrons of $E > 12$ Mev could get through the 6 gm/cm^2 shielding into the nuclear emulsions. No electrons were found, but a large number of protons were found. The energy spectrum of protons measured by Freden and White on a later flight (Reference 32) is shown in Figure 5. Other experiments (References 33, 34, 35, and 36) have shown very similar energy spectra and intensities of protons and have extended the data down to lower energies. Below about 40 Mev the energy spectrum becomes quite flat and shows a slight dip at about 20 Mev. The inner-belt proton flux seems quite constant in time, varying by less than a factor of 2 for several flights. This indicates that the particle lifetime is quite long.

Calculation of the Energy Spectrum

We can get a quantitative picture of the flux and energy spectrum of the inner-radiation-belt protons produced by neutron β decay by considering the conservation of particles. The continuity equation in energy space can be written (Reference 37)

$$\frac{dN(E)}{dt} = S_p(E) - L(E) + \frac{\partial}{\partial E}\left[J(E)\right] , \qquad (21)$$

where $N(E)$ is the equilibrium-proton-density energy spectrum, $S_p(E)$ is the source of protons, $L(E)$ is the loss term, and $J(E)$ is the "energy current" = $N(E)\, dE/dt$ for equilibrium $dN(E)/dt = 0$. Let us now consider two special cases of this equation for equilibrium.

Case A: $L(E) = 0$.

For protons between 5 and 100 Mev the dominant loss process is slowing down by exciting and ionizing electrons by distant coulomb collisions, and we can ignore other losses. This slowing down contributes to the energy-current term and is not considered here to be part of $L(E)$; Equation 21 becomes now

$$S_p(E) = \frac{\partial}{\partial E}\left[N(E)\frac{dE}{dt}\right] . \qquad (22)$$

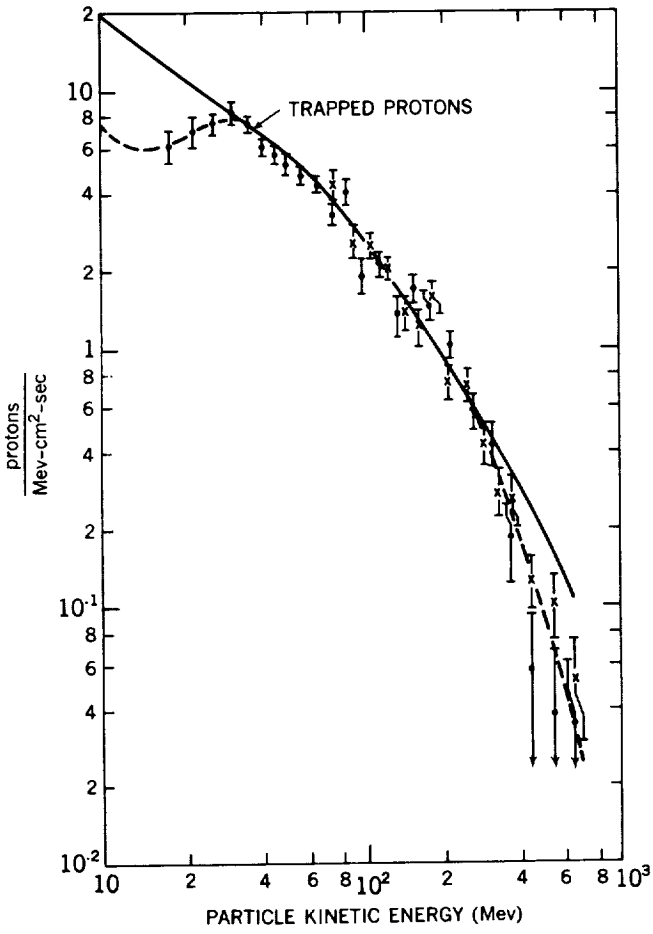

Figure 5—The spectrum of trapped high-energy protons at 1100 km measured by Freden and White. Reproduced with permission from Reference 32. The solid dots are data from a flight on October 13, 1960, and the crosses are from a flight in April 1959 normalized to the other at 100 Mev. The solid curve is the theoretical proton curve. The dashed curve is a fit to the high-energy data.

The proton-source term is given by the neutron's decay density from equation 17:

$$S_p(E) = \frac{dn(E)}{dV} = \frac{\eta\, 0.8\, E^{-2.0}}{\gamma v \tau_n}\left(\frac{R_e}{R_e + h}\right)^3 . \qquad (23)$$

This expression is valid at low latitudes and close to the earth. The coefficient η is put in here because not all of the neutrons that decay form protons that are trapped (Reference 38). Some of the protons made by neutron decay have pitch angles that are so small that they will hit the earth before they mirror. These protons will not form part of the trapped radiation. The coefficient η is called an injection coefficient and gives the fraction of protons that are trapped. The average value of η for inner-belt protons is $\bar{\eta} \approx 0.30$ (Reference 39).

We can solve Equation 22 approximately (References 33 and 40) for the energy range 10 to 80 Mev by writing $dE/dt = v\, dE/dx$ and approximating $dE/dx = 243\, \rho E^{-0.79}$ Mev/cm; $v = 1.45 \times 10^9 \times E^{0.477}$ cm/sec; and $\gamma = 0.93\, E^{0.32}$, where ρ is the air density in gm/cm^3. Substituting in Equation 22 we get

$$\frac{(0.30)(0.8E^{-2.0})\left(\frac{6400}{7500}\right)^3}{(0.93E^{.032} \times 1.45 \times 10^9 E^{0.477} \times 1000)} = \frac{\partial}{\partial E}\left[kE^{-n}\, 243\, \rho E^{-0.79} \times 1.45 \times 10^9 E^{0.477}\right]. \qquad (24)$$

Solving this gives

$$\Phi(E) = \nu N(E) = k E^{-n} = \frac{2.9 \times 10^{-16}}{\rho} E^{-0.72} \quad \text{for } 10 \text{ Mev} < E < 80 \text{ Mev}. \qquad (25)$$

If a time-averaged density of $\rho = 2.8 \times 10^{-18}$ gm/cm^3—corresponding to an atomic density of 1.0×10^5 atoms/cm^3—is used, then $\Phi(E) = 110\, E^{-0.72}$ protons/cm^2-sec-Mev. This density is quite reasonable for this situation. The diurnal average density at 1100 km near solar maximum is about 2.5×10^5 atoms/cm^3 (Reference 41). The time-average density along a particle orbit is less than this by about a factor 2 (Reference 42), so the density used is quite a good one. This expression for $N(E)$ fits the Freden and White data well.

The lifetime τ_p of these protons can be obtained by using the "leaking bucket" equation (Reference 12). We have for this problem, for equilibrium,

$$\text{Input} = \text{Output} = \frac{\text{Contents}}{\tau_p}, \qquad (26)$$

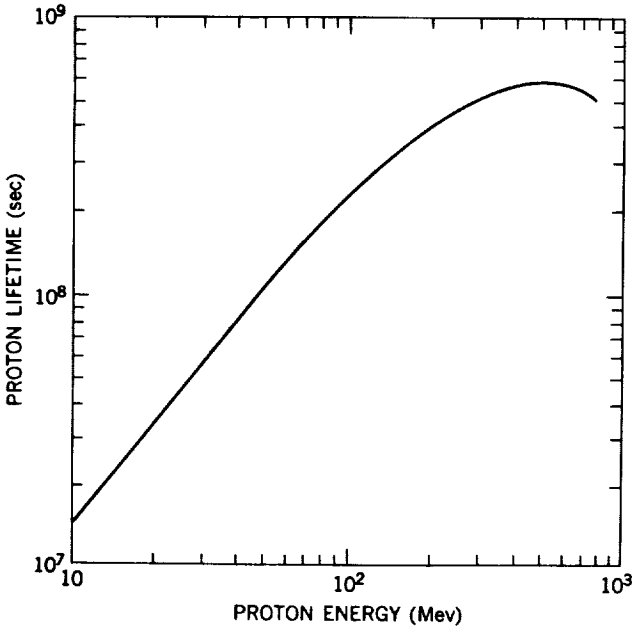

Figure 6—Proton lifetimes at 1100 km in the inner belt based on slowing down and nuclear collisions.

which gives

$$\tau_p = \frac{\text{Contents}}{\text{Input}} = \frac{N(E)}{S(E)}.$$

We know $S(E)$ from Equation 23 and $N(E)$ from the solution of Equation 24 (shown as the solid curve on Figure 5); we can therefore calculate the lifetime directly. This gives $\tau_p = 7.0 \times 10^5\, E^{1.3}$ sec for 10 Mev $< E <$ 80 Mev for 1100 km altitude. Figure 6 shows values of τ_p. For other oxygen densities the lifetime τ_p varies inversely as the time average density.

Case B: $dE/dx \approx 0$.

If some other loss process occurs considerably faster than slowing down, then the protons

will have essentially constant energy; slowing down can then be neglected. This situation is approximated for protons of $E > 300$ Mev. For these energies, the protons almost all have nuclear collisions before they slow down. The cross section σ for an inelastic collision of a high-energy proton with an oxygen nuclei is 3.0×10^{-25} cm^2. This gives a mean free path for nuclear interactions of $\lambda = \rho/n\sigma = 2.67 \times 10^{-23}$ gm/atom $/ 3.6 \times 10^{-25}$ cm^2/atom $= 74$ gm/cm^2. The range of a 500 Mev proton in oxygen is 135 gm/cm^2; therefore, these high-energy protons will usually have nuclear collisions before slowing down much. In this case, Equation 21 becomes

$$S(E) = L(E) \tag{27}$$

For the loss term here we can write

$$L(E) = N(E)\, n \sigma \nu \ , \tag{28}$$

where n is the atomic density in atoms/cm^3; this gives

$$N(E) = \frac{\eta\, 0.8\, E^{-2.0} \left(\frac{R_e}{R}\right)^3}{\gamma \nu \tau_n} \left(\frac{1}{n \sigma \nu}\right) . \tag{29}$$

When we substitute

$$\nu = 2.69 \times 10^9\, E^{0.344} \ ,$$

$$\gamma = 0.428\, E^{0.205} \ ,$$

$$n = 1.0 \times 10^5 \text{ atoms/cm}^3 \ ,$$

$$\sigma = 0.36 \times 10^{24} \text{ cm}^2 \ ,$$

which are valid for 80 Mev $< E <$ 700 Mev, Equation 29 becomes

$$\Phi(E) = \nu N(E) = 4.2 \times 10^6\, E^{-2.54} \frac{\text{protons}}{\text{cm}^2\text{-sec-Mev}} . \tag{30}$$

This is an asymptotic expression for $N(E)$ at high energies where slowing down is not important. Above 300 Mev it holds quite well but below this slowing down also is important.

The general form of Equation 21 has been solved (Reference 33) to give the solid curve in Figure 5. The form of the solid curve above 300 Mev agrees well with Equation 30, and below 80 Mev the curve is exactly given by Equation 25. There is no arbitrary normalization involved here; there are

no adjustable parameters in the theory—the comparison of experiment and calculation is direct. We know the source strength and properties, we know the loss processes and rate, and we know the properties of the atmosphere: from these data we get directly the proton-energy spectrum. The agreement with the data here is so good that the analysis is quite certainly correct, and neutron decay is the source of these protons.

Spatial Distribution

The spatial distribution of the inner-belt protons was first measured by the GM counter in Explorer IV (Reference 10). When these data were obtained it was not known that the counting rate of this detector was due to protons, but it is now quite certain that this is the case. The 302 GM counter on board counted protons of $E_p > 30$ Mev and electrons of $E_e > 3$ Mev. The electron flux above this 3 Mev energy limit in the inner belt is thought to be quite small.

Contours of constant count rate measured on Explorer IV by Van Allen are shown in Figure 7. The count rates increase with altitude, and show a fairly complicated change with latitude and longitude. Figure 8 gives curves (taken from Reference 43) of the increase of count rate with altitude at different locations. The data curves O_1 and O_2 were obtained near Singapore; E_1, E_2, and E_3 near Nigeria, Africa; A_1 in northern South America; and A_2 and A_3 in central South America. All of these locations are at about the same magnetic latitude, but the curves show quite different altitude behaviors. The reason for this is that the earth's surface magnetic field is different at these different locations. When these data are replotted in terms of the magnetic field instead of altitude at each location (Figure 9) the curves then become essentially indistinguishable (Reference 43). The reason for this is

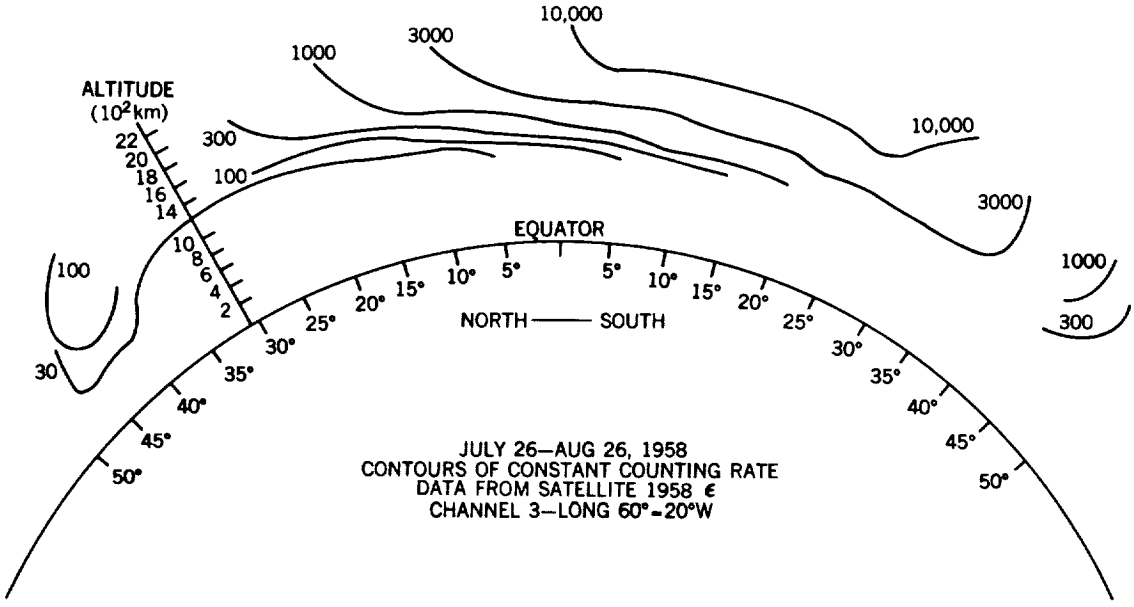

Figure 7—A meridian section through the earth showing observed contours of the count rate of the unshielded GM tube on the Explorer IV satellite for the period July 26 to August 26, 1958, within longitude range 80° ± 20°W. Reproduced with permission from Reference 10.

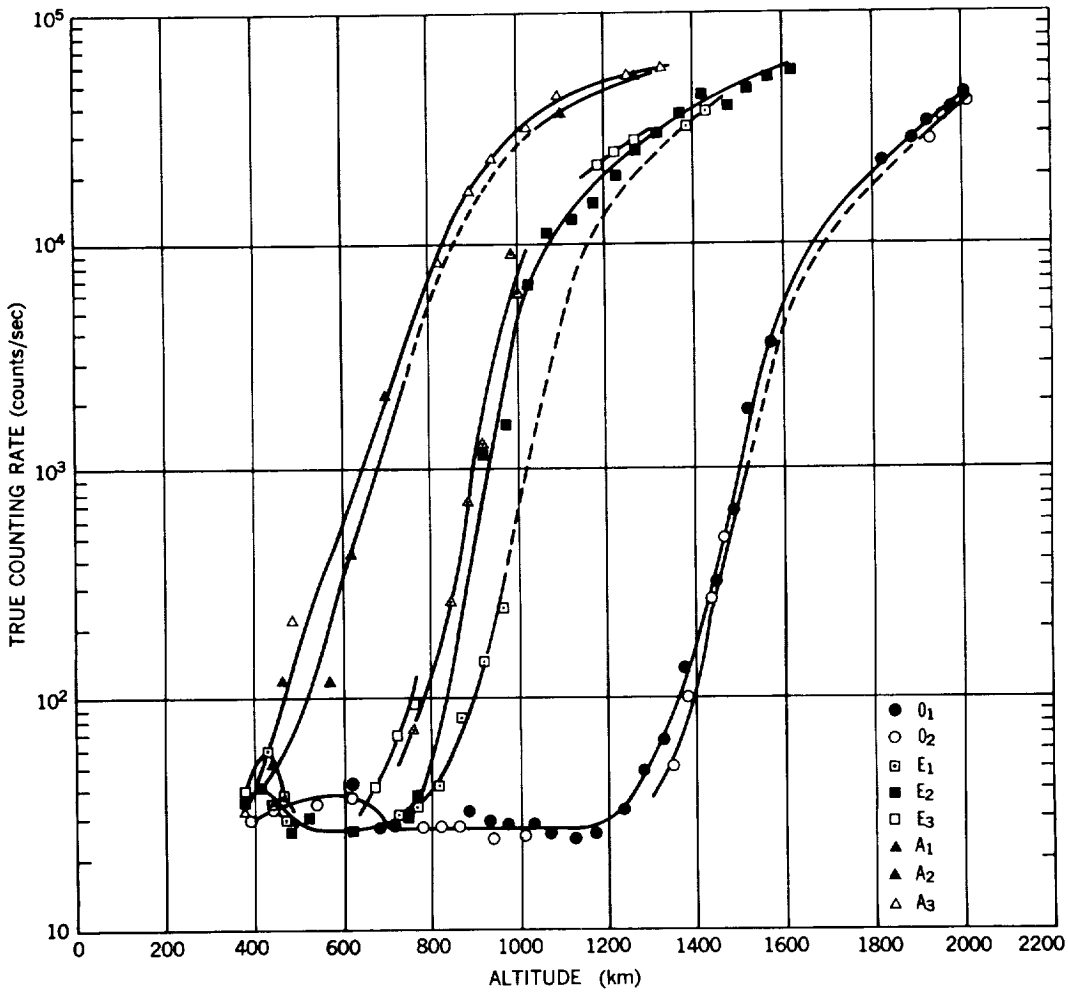

Figure 8—Counting rate as a function of altitude for the GM counter on the Explorer I satellite for several different positions near the magnetic dip equator. The curves labeled "O" are data near Singapore, those labeled "E" are near Nigeria, the A_1 curve is in Northern South America and A_2 and A_3 are in Central South America. Reproduced with permission from Reference 43.

easily understood in terms of the motion of charged particles in a dipole magnetic field. The particles bounce back and forth, mirroring at one particular value of the magnetic field B. The particles also drift around the earth staying on a surface of constant integral invariant I; this corresponds to staying at a constant magnetic latitude. Therefore, for observations at one latitude the count rate should vary with B as it does in Figure 8. The altitude of the mirror points represented by the count rates in Figure 8 get as low as 400 km over South America. Below this altitude, galactic cosmic rays provide most of the count rate. The lower edge of the trapped radiation belt is clearly controlled by the atmosphere. Protons are lost by slowing down. A 50 Mev proton, to be brought to rest, must transit about 2.5 gm/cm^2 of oxygen. At 400 km, the atmospheric density is about 5 x 10 atoms/cm^3 or about 10^{-14} gm/cm . At velocity of 10^{10} cm/sec, the proton will take about 2 x 10^4 sec to slow to a stop. But, because of the variations or atmospheric density along the particle's orbit—especially the variation due to the drift in longitude—the lifetime is increased probably to 10^6 sec. The source

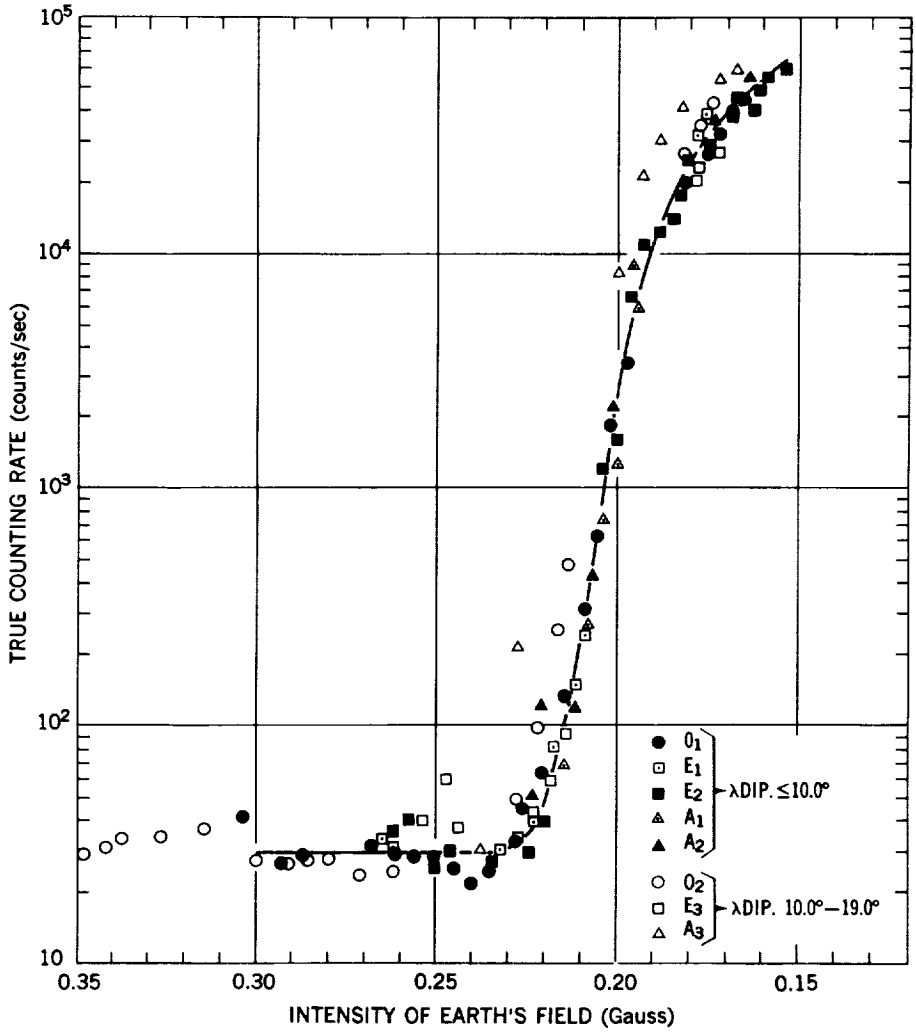

Figure 9—The same counting rate data as shown in Figure 8 replotted in terms of computed magnetic field strength at the observing point. All of the curves from Figure 8 are now essentially superimposed. Reproduced with permission from Reference 43.

strength of fast protons from neutron decay near the earth is about 10^{-15} protons/cm^3-sec but perhaps only 30 percent of these will be going in the proper direction to be trapped. We get an equilibrium flux here of

$$\Phi_p = \left(0.3 \times 10^{-15} \frac{\text{protons}}{\text{cm}^3\text{-sec}}\right)\left(10^{10}\frac{\text{cm}}{\text{sec}}\right)\left(10^6 \text{ sec}\right) = 0.3\frac{\text{protons}}{\text{cm}^2\text{-sec}} .$$

This calculation is not very exact, but the value of the flux thus found is comparable with the cosmic-ray flux of about 2 protons/cm^2-sec; therefore, it is reasonable that below this altitude of 400 km the trapped flux gets too small to be measured and cosmic rays dominate.

We are quite certain the lower edge of the inner belt of high-energy protons is controlled by the earth's atmosphere. But we are not nearly so certain what controls the outer edge of the proton belt. We would expect, from what is known of the inner belt, that it should extend out many earth radii. The neutron decay source strength decreases about as $1/R^4$, but the proton lifetime for slowing down should go up about as fast as the source strength goes down, so the equilibrium proton flux expected in the outer belt is about the same as that observed in the inner belt. Actually, the observed trapped high-energy proton flux in the outer belt is less than the cosmic-ray flux and consistent with zero. Fan, Meyer and Simpson (Reference 44) gave an outer-belt proton flux of

$$\Phi_p = 0 \pm 0.1 \frac{\text{protons}}{\text{cm}^2\text{-sec}} \text{ for } E_p > 75 \text{ Mev.}$$

This means that the lifetime of the protons in this region is reduced by a factor of 10^4 or more by some additional process.

The processes which seem most probable to cause this reduction in lifetime have to do with time variations of the magnetic field. Welch and Whitaker (Reference 45) suggested that time or space variations in the magnetic field could produce "magnetic scattering" of trapped particles. If the magnetic perturbations are of such character that they cause a breakdown of the adiabatic invariants then the particle's motion will be altered. Hydromagnetic (hm) waves having a wave length $\lambda < R_c$, where R_c is the particle cyclotron radius, will break down the magnetic moment invariant. When the particle encounters the wave a change in μ will take place, and as the result the particle's mirror point will be changed. Repeated encounters with waves will cause a diffusion of the particle's mirror point and result in a loss of particles out of the loss cones into the atmosphere.

Dragt (Reference 46) has calculated the effect of hydromagnetic waves on a high-energy proton magnetic moment. He finds that for hm wave frequencies of a few cps and for particles traveling along field lines, a condition can exist such that the hm wave frequency is Doppler shifted to equal the particle's cyclotron frequency. For this resonant condition the particle's magnetic moment is changed as a result of interacting with the wave.

The particle lifetime τ against hm wave scattering is given by Dragt as

$$\tau = \frac{2\tau_B}{\pi^2 p^2}\left(\frac{\Delta B_{hm}}{B}\right)^2 , \tag{31}$$

where τ_B is the bounce period and p is the number of hm waves encountered per bounce. For 100 Mev protons at $2R_e$ the bounce period $\tau \approx 0.1$ sec, and B = 0.04 gauss. Assuming $\Delta B = 3$ gamma and $p = 1$ we get

$$\tau \approx \frac{1}{2} \text{ day.}$$

This lifetime is short enough that the equilibrium flux of protons in the outer belt would not be measured because the cosmic-ray flux is larger.

Also, the radial dependence of the scattering is reasonable. At $2R_e$, the maximum energy trapped is proportional to R^{-11}. But at smaller altitudes, the scattering is less. The count rate versus altitude curve of the GM counter on Pioneer III is reasonably well reproduced by this analysis. The requirements on hm wave characteristics here are quite reasonable. A wave characteristic of $\Delta B = 3\gamma$ at 3 cps is not a very large disturbance.

Wentzel (Reference 47) made a similar analysis of the breakdown of the magnetic moment of high-energy protons by hm waves. He found that the magnetic moment was changed for encounters with hm waves when $v/v_c > 0.4$, where v_c = hm wavelength/larmor period. Accordingly, 56 Mev protons should extend out to 6000 km and 28 Mev protons out to 7000 km. These results are relatively similar to Dragt's results.

Parker (Reference 48) has considered how a breakdown of the integral invariant I can transport and accelerate particles. If the magnetic field at the mirror point changes in a time short compared to a bounce period, then I is not a constant of the motion. The bounce period is (Reference 49)

$$\tau_B \approx \frac{4r_0}{v} \approx \frac{4 \times 10^9 \text{ cm}}{10^{10} \frac{\text{cm}}{\text{sec}}} = 0.4 \text{ sec.} \tag{32}$$

So, waves having a frequency of 5 or 10 cycles/sec will cause nonadiabaticity here. These waves at the mirror point result in a Fermi acceleration (Reference 50). Some particles encounter mirror points moving towards them due to the field perturbation ΔB and some particles find mirror points moving away from them. But, because statistically more approaching collisions take place, there is a net energy gain given by

$$\frac{dE_{\parallel}}{dt} = 8E_{\parallel}\left(\frac{v}{\omega_{\parallel}}\right)^2 p \, , \tag{33}$$

where $E_{\parallel}$ and $\omega_{\parallel}$ are the particle energy and velocity component along the field line, respectively, p is the number of mirror point reflections per unit time, and v is the velocity of the mirror point motion.

The interesting feature here is that as the particle gains energy its mirror point is systematically lowered because all the energy gain is in $E_{\parallel}$ and, therefore, the pitch angle decreases and the particle is lost into the atmosphere. For a $\Delta B/B$ of 10^{-3} and constantly moving mirror points, the characteristic time for a particle to diffuse down into the atmosphere is about 3×10^6 sec. It is not known whether these hydromagnetic wave conditions are really met, and thus whether this lifetime is reasonable or not. Parker made this analysis for outer-belt 100 kev electrons, but it applies equally to protons of about 50 Mev.

A proton lifetime of 3×10^6 seconds and a source strength of about 0.2×10^{-15} protons/cm^3-sec gives an equilibrium flux of

$$\Phi_p = \left(0.2 \times 10^{-15} \frac{\text{protons}}{\text{cm}^2\text{-sec}}\right)\left(10^{10} \frac{\text{cm}}{\text{sec}}\right)\left(3 \times 10^6 \text{ sec}\right) = 6 \frac{\text{protons}}{\text{cm}^2\text{-sec}} \, .$$

But this is larger than the measured outer-belt flux by at least an order of magnitude, so the lifetime must be less than 10^6 sec by a factor of 10 or more. From this analysis it seems that the breakdown of the integral invariant probably is not the dominant loss process, but that another process gets rid of the protons faster.

It would appear from the work of Dragt (Reference 46) and Wentzel (Reference 47) that the breakdown of the magnetic moment of the protons by hm waves caused the loss of protons in the outer belt. The hm waves required to do this seem available and the results of the calculations agree reasonably well with observations. We cannot be sure that hm wave scattering is the controlling factor for the outer edge of the inner belt because there is no direct verification of this, but it seems the best guess now.

If the outer edge of the proton belt is controlled by hm wave scattering as we think, then there may be an interesting solar cycle change in the proton flux at $2R_e$ and beyond (Reference 46). If, at solar minimum, there is less energy in hm waves (as seems reasonable), then the proton lifetime will increase and an appreciable flux of protons may build up in the outer belt.

In order to organize the kind of data shown in Figure 7 into some easily manageable form, McIlwain developed the B-L coordinate system (Reference 51) where B is the scalar magnetic field and L is a distance which, in a dipole field, is the distance to the equator for a particular field line. It is defined in terms of the integral invariant I in such a way that the real earth's field is used. L is very nearly constant along a field line, so it can replace the commonly used equatorial radius R_0, but use real values of the earth's field. The Explorer IV data in Figure 7, when plotted in terms of B-L coordinates, can be combined for different geographic latitudes, longitudes, and altitudes into the simple form shown in Figure 10. Reading down a line of constant L here corresponds to going out from the earth along a field line. This information can be transformed into a more familiar form by using

$$R = L\cos^2\lambda ,$$

and

$$B = \frac{M}{R^3}\sqrt{4 - \frac{3R}{L}} .$$

This R, λ presentation of the data in Figure 11 has the earth's magnetic field transformed into a dipole field, but the earth's surface now has an odd shape.

Figure 11 is a representation of the fluxes of high-energy protons ($E_p > 30$ Mev) in the inner belt as of 1958. It is probably accurate to within a factor 2 over most of the range of values. The picture was somewhat different in 1961; this variation is discussed later.

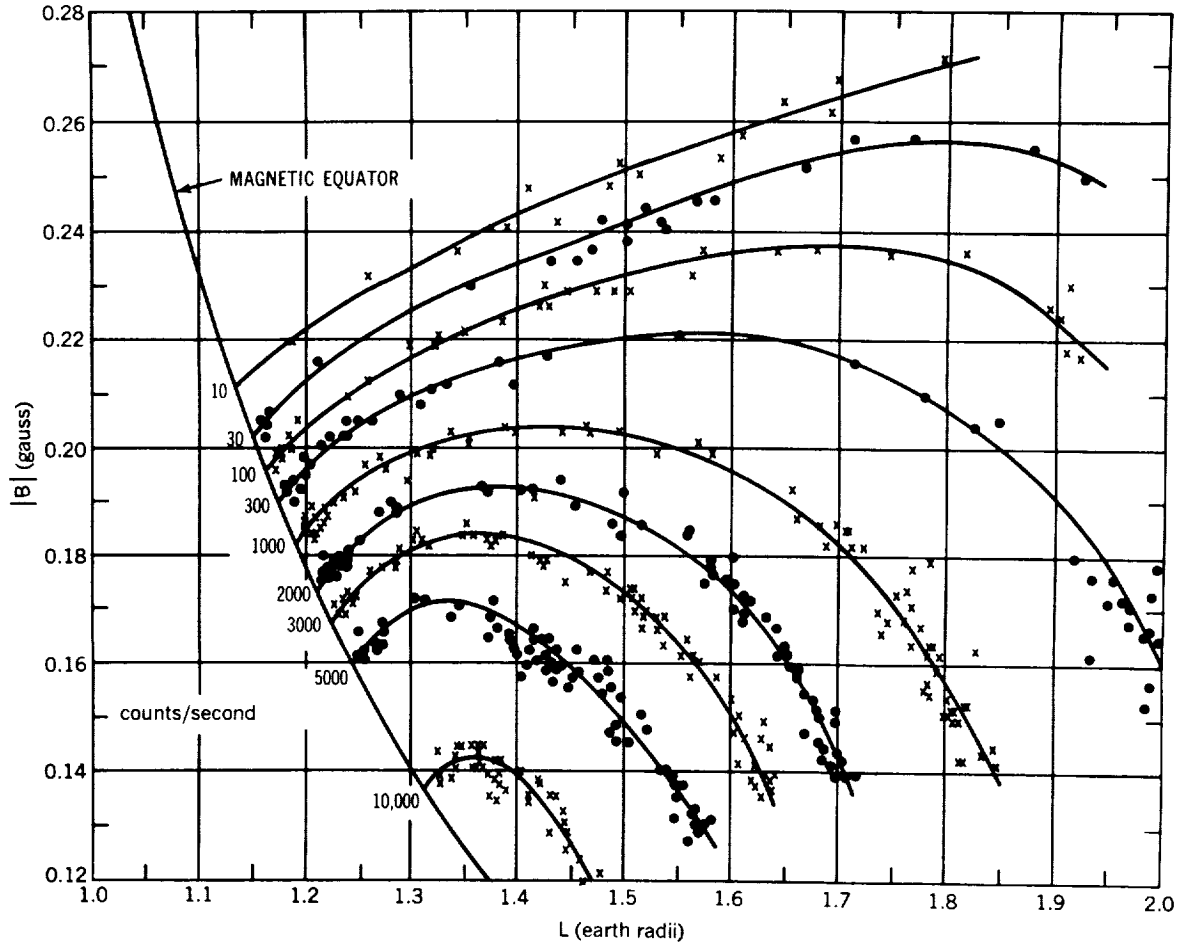

Figure 10—Contours of constant true counting rate of the unshielded GM counter in Explorer IV. The points shown correspond to data obtained over a wide range of geographic latitude and longitude. Reproduced with permission from Reference 51.

In Figure 11, the data from Explorer IV have been combined with data from Pioneer III to extend the range of B-L values covered. This, with some extrapolations, covers the whole inner belt. The count rates in Figure 10 have been converted to particle fluxes in Figure 11 by the use of the proper detector geometrical factors.

Pioneer III went out radially about 100,000 km from the earth and then returned (Reference 12). It cut through the inner belt twice. The 302 GM counter on board was nearly identical in threshold to the counter in Explorer IV; however, it had a slightly larger geometrical factor $G_0 = 0.62$ (Reference 12). The count rate curve for the reentry flight is shown in Figure 12. The section from 15,000 km inwards is the important region for us. This shows the nature of the outer edge of the proton belt within about 20 degrees of the equator and, when combined with Explorer IV data, allows us to make a more complete map of the inner-belt-proton flux.

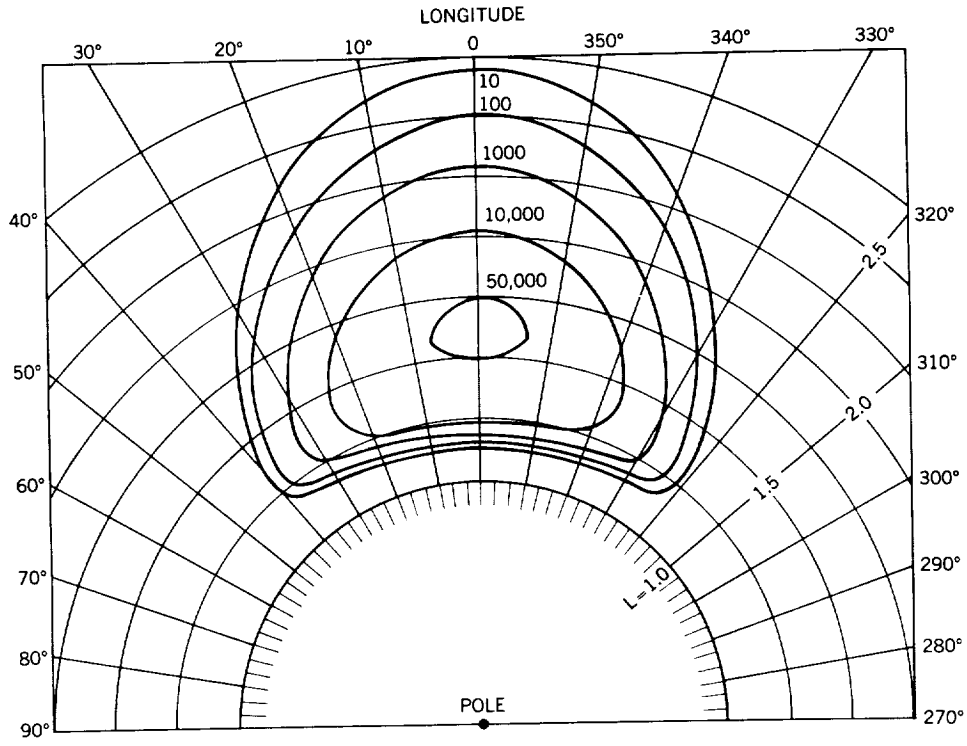

Figure 11—High-energy-proton fluxes in the inner belt. This is a R-λ representation based on McIlwain's L parameter. On this picture the earth's surface is bumpy, but centered on L = 1. The fluxes are given in protons/cm^2-sec.

Time Variations

The protons in the inner radiation belt show relatively small changes in intensity with time in contrast to the outer belt, which varies considerably, especially at the time of magnetic storms.

Changes in the proton flux at low altitudes were not seen even in connection with magnetic storms on Explorer IV (Reference 52). There may be some small time changes in the proton energy spectrum: a small peak at about 75 Mev seemed to be present in the proton energy spectrum measured in July 1959 (Reference 37); then in October 1960 a peak was observed at 30 Mev (Reference 32). There is a

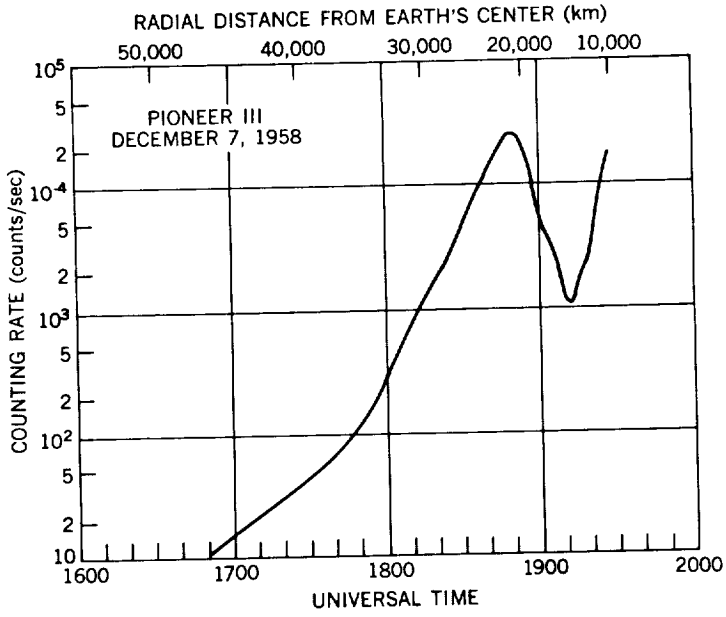

Figure 12—True count rate of the 302 GM counter on Pioneer III on the inbound flight. Reproduced with permission from Reference 12.

possibility that it is the same peak degraded in energy, and that it was the result of neutrons produced in one polar cap proton event (Reference 53). There is little doubt that polar cap protons are important in generating neutrons, but it seems questionable whether this structure in the trapped proton energy spectrum is the result of polar cap protons. It now appears that if there are changes in the spectral shape above 30 Mev, they are quite small (Reference 32).

Time changes in the inner belt have been detected by the 302 GM counter on Explorer VII (Reference 55). It counted protons of $E_p > 18$ Mev and electrons of $E_e > 1.1$ Mev. At the outer edge of the inner belt for $1.8 < L < 2.2$ time variations of a factor of 3 or more are seen at the times of magnetic storms. The changes may well be in the electron population. For $1.5 < L < 1.8$ there are small variations seen in the count rate at storm times, maybe in the proton population or maybe not.

From November 1959 to November 1960 a rather gradual increase of a factor of 2 in intensity was seen in the inner part of the inner belt ($L < 1.5$) by Explorer VII. At least part of this increase is expected, on two grounds: (1) the cosmic-ray flux increases by about a factor of 2 from solar maximum to solar minimum, and (2) the exospheric densities will decrease. The heating of the exosphere is less at solar minimum, so that the scale height decreases and therefore the densities decrease.

Recent calculations on the solar cycle change of exospheric density (Reference 41) give the atomic densities listed in Table 3.

Table 3

Atomic Densities at Various Altitudes.

Altitude (km)	Atomic Densities (atoms/cm^3)			
	Near Solar Maximum†		Near Solar Minimum††	
	N(O)	N(He)	N(O)	N(He)
1000	7×10^5	4.4×10^5	440	1.1×10^5
1500	1.1×10^4	1.6×10^5	18	1.6×10^4
2000	290	6.2×10^4	0	2800

†S = 200 from Reference 41.
††S = 70 from Reference 41.

Both the slowing down loss process and the nuclear collision loss process will vary with these two densities. The slowing down rate dE/dx goes as

$$\frac{dE}{dx} \propto \left[4\,N(O) + N(He)\right] .$$

Oxygen is more important here because it has 4 times as many electrons to help in slowing down. The nuclear collision rate C shows a similar variation

$$C \propto \left[2.5\,N(O) + N(He)\right] .$$

The oxygen nucleus has a large cross section σ for nuclear collisions $(\sigma \propto A^{2/3})$, so oxygen has more collisions per nucleus than helium does.

From Figure 6 we got the proton lifetime at 1000 km altitude for near solar maximum given in Table 4. The other values in the table are obtained from these 1000 km values by using density variations in Table 3 and Equation 26.

Table 4

Inner Belt Proton Lifetimes.

Energy (Mev)	Lifetime					
	Near Solar Maximum (sec)			At Solar Minimum (sec)		
	1000 km	1500 km	2000 km	1000 km	1500 km	2000 km
15	2.4×10^7	3.8×10^8	1.4×10^9	7.2×10^8	4.8×10^9	2.4×10^{10}
40	8.5×10^7	1.2×10^9	5.2×10^9	2.5×10^9	1.7×10^{10}	8.4×10^{10}
100	2.8×10^8	4.2×10^9	2.0×10^{10}	8.4×10^9	5.6×10^{10}	2.8×10^{11}

The period of the solar cycle $\tau_{sc} = 4 \times 10^8$ seconds. If the proton lifetime is short compared to this, then the particle population will change with changes in source strength or loss rate; but if the proton lifetime is long compared to τ_{sc}, then the solar cycle will be averaged out and no population changes will occur. We see from Table 4 that changes in low-energy particles at 1000 km will be appreciable, but at 2000 km no changes will occur. The factor of 2 increase in the number of protons of $E_p > 19$ Mev seen by Explorer VII at 1000 km during 1960 (Reference 54) is consistent with the increase expected here on the basis of solar cycle changes in cosmic ray flux and exospheric density.

MEDIUM-ENERGY PROTONS

Out to about $L = 1.6$, the proton energy spectrum is as shown in Figure 5; but for $L > 1.7$, Naugle and Kniffen (Reference 35) found that for $E_p < 30$ Mev the spectrum showed a sharp rise above this curve. Apparently some additional process comes into play to produce these protons of $E_p < 30$ Mev near the outer edge of the inner belt. The Naugle and Kniffen data are given in Figure 13.

A second experiment apparently saw this same group of particles: A proton spectrometer flown on a Scout vehicle to an altitude of 4800 km found a large number of protons (Reference 55) of 1 Mev $< E_p <$ 10 Mev. One part of Naugle and Kniffen's data was at 1884 km altitude at $L = 1.722$ and could be fit well by

$$\Phi_p(E) = 6.8 \times 10^6 E^{-4.5} \frac{\text{protons}}{\text{cm}^2\text{-sec-ster-Mev}} \text{ for } 10 \text{ Mev} < E_p < 50 \text{ Mev.}$$

Bame, et al. (Reference 55) made measurements at 4800 km at $L = 2.50$ and got a proton flux given by

$$\Phi_p(E) = 2 \times 10^6 E^{-5.2} \text{ for } 1 \text{ Mev} < E_p < 2.24 \text{ Mev}$$

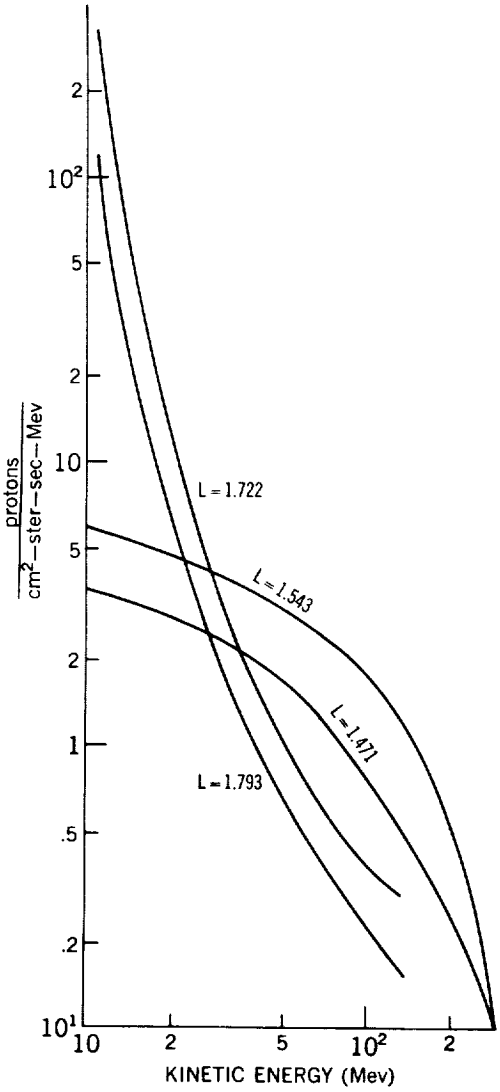

Figure 13—Proton-energy spectra measured by Naugle and Kniffen for different positions along the vehicle trajectory. Reproduced with permission from Reference 35.

and

$$\Phi_p(E) = 0.71 \times 10^6 E^{-3.9}$$

for 2.2 Mev < E_p < 7.3 Mev.

Bame, et al. showed that an extrapolation of the Naugle-Kniffen data down to 1 Mev gave moderately good agreement with their data (see Figure 14). Therefore, it appears that these two experiments were observing the same type of particles.

What new source of particles can produce medium-energy trapped protons only above L = 1.7? Armstrong, et al. (Reference 34) suggested that solar protons bombarding the polar cap at the time of solar flares should produce neutrons, and that the decay of these neutrons then constitutes a new source of protons. We are sure that galactic cosmic ray protons produce neutrons which then produce inner belt protons; so it seems very reasonable that solar protons should similarly produce neutrons and thereby trapped protons.

The trapped protons produced from solar protons will be different from the other trapped protons in two ways. First, their spatial distribution will be different. This is because solar protons arrive at the earth only in the polar regions (because of their low energy, the earth's field prevents them from getting further from the poles than about 55 degrees of magnetic latitude). The inner part of the inner belt is therefore geometrically shadowed from this source, so more of these neutrons can produce trapped protons near the inside of the inner belt. Lenchek (Reference 56) has calculated that no trapped protons will be produced for L < 1.65. This is consistent with the data of Naugle and Kniffen (Reference 35).

The second distinctive feature of trapped protons produced from solar protons is that the intermediate neutrons produced this way have lower average energies than those from the galactic cosmic ray source. The solar proton energy spectrum usually extends up past 100 Mev, but most of the protons have much lower energies. Therefore, the neutron energy spectrum will not contain many

particles of E > 50 Mev and the peak of the neutron spectrum should be at about 1 Mev. Lenchek (Reference 56) approximated this neutron spectrum $S_n(E)$ by an evaporation spectrum

$$S_n(E) = kEe^{-E/4},$$

and evaluated the total flux of trapped protons made by this process.

A 10 Mev proton that mirrors at 1500 km has a lifetime for slowing down of about 10 years, so this process will average over a large number of solar events. Lenchek estimated the time-average solar-proton flux from data of Webber (Reference 57) to be about 10 protons/cm^2-sec-ster, which is much higher than the galactic cosmic ray flux. Using an average atmospheric density of 10^3 atoms/cm^3, he obtained the trapped-proton flux observed by Naugle and Kniffen (Reference 35). These numbers seem a little extreme, but the idea seems completely reasonable.

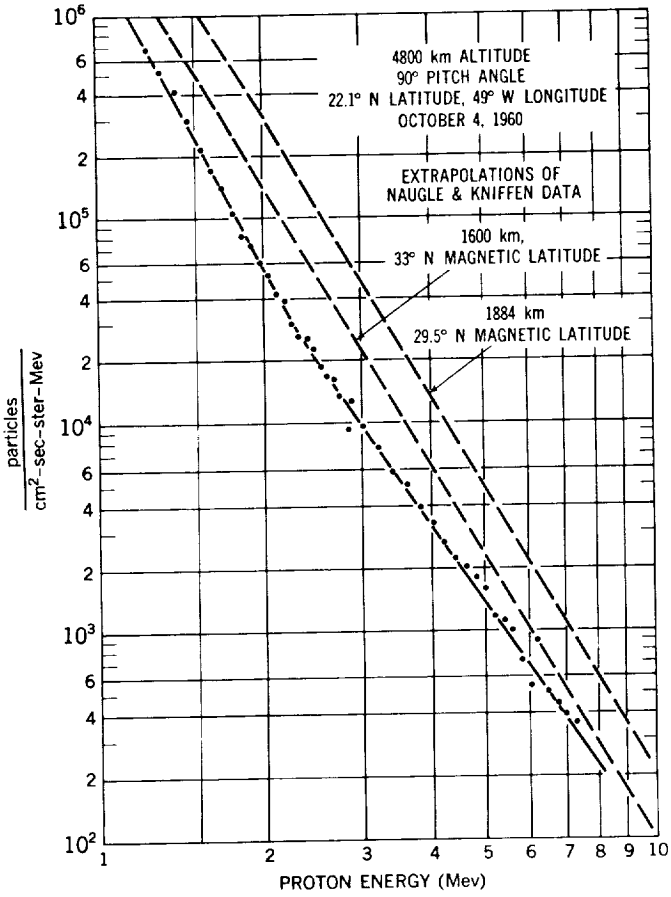

Figure 14—Energy spectrum at 4800 km for protons measured by Bame, Conner, et al. Two of the spectra obtained by Naugle and Kniffen have been extrapolated to lower energies and are shown. Reproduced with permission from Reference 55.

It appears quite reasonable from this analysis that these low-energy protons are made from solar protons striking the polar atmosphere. The fact that there is a sharp inner edge on this type of trapped radiation strongly rules against direct solar injection or local acceleration (Reference 56).

LOW-ENERGY PROTONS

One of the most interesting recent radiation-belt discoveries is the large flux of low-energy protons at 1000 km (Reference 58). On Injun, a CdS detector measured a heavy ion energy flux of about 30 ergs/cm^2-sec-ster at 1000 km in the energy range of 0.5 kev to 1 mev. These particles are probably protons. If they have an average energy of 100 kev, there is a proton flux of

$$\Phi_p = \frac{\left(50 \frac{\text{ergs}}{\text{cm}^2\text{-sec-ster}}\right)(1 \text{ ster})}{\left(0.1 \frac{\text{Mev}}{\text{proton}}\right)\left(1.6 \times 10^8 \frac{\text{erg}}{\text{Mev}}\right)} = 3 \times 10^8 \frac{\text{protons}}{\text{cm}^2\text{-sec}} .$$

This is a quite large flux. The spatial distribution of these low-energy protons is very similar to the distribution of high-energy inner-belt protons.

This strong similarity might be explained by: (1) the two groups of particles coming from a common source, (2) the high-energy protons generating the low-energy protons. We are very sure the high-energy protons are made by neutron decay. Also, slow protons produced by neutron decay do exist. We can evaluate the possibility that the observed slow proton flux results from neutron decay. Most of the neutrons in the leakage spectrum are between 100 kev and 10 Mev. Let us say that one half of the neutron-decay events at 1000 km produce protons of about 1 Mev. From Figure 3 we see that about 2×10^{-12} protons/cm^3-sec will be made in the Mev range from these decay events. If these protons are lost by slowing down, they must encounter 3×10^{-3} gm/cm^2. In an atmosphere of $n = 2.5 \times 10^5$ O atoms/cm^3 of oxygen (or $\rho = 6 \times 10^{-18}$ gm/cm^3), and traveling at an average velocity of 5×10^8 cm/sec during the slowing down process, a 1 Mev proton will slow down in a time τ given by

$$\left(6 \times 10^{-18} \frac{\text{gm}}{\text{cm}^3}\right) \left(5 \times 10^8 \frac{\text{cm}}{\text{sec}}\right) \tau = 3 \times 10^{-3} \frac{\text{gm}}{\text{cm}^3}$$

or

$$\tau = 10^6 \text{ seconds} .$$

We get from this the equilibrium-proton flux of

$$\Phi_p = \left(2 \times 10^{-12} \frac{\text{protons}}{\text{cm}^3\text{-sec}}\right) \left(5 \times 10^8 \frac{\text{cm}}{\text{sec}}\right) (10^6 \text{ sec}) = 10^3 \frac{\text{protons}}{\text{cm}^2\text{-sec}} .$$

This is much less than the observed flux of $\Phi_p \approx 10^8$ so this process can not produce the observed protons.

Next, we can consider the possibility that the high-energy protons produce the low-energy protons. This might be done by coulomb collisions with the thermal protons. We can estimate the flux produced in this way. The cross section for coulomb collisions is

$$d\sigma = e^4 \frac{2\pi \sin\theta \cos\theta \, d\theta}{E^2} \left(\frac{1}{\sin^4\theta}\right) , \tag{34}$$

where E is the energy of the incident particle and θ is the scattering angle. For a range of values of θ, the struck proton will have energies E_s in the 0.5 kev to 1 Mev energy range given by

$$E_s = E \sin^2\theta . \tag{35}$$

Integrating over θ to get the total cross section and rearranging the coefficient gives

$$\sigma = \frac{0.5 \times 10^{-24}\ \text{cm}^2}{\left(\frac{E}{mc^2}\right)^2} \int \frac{d \sin\theta}{\sin^3\theta} = \frac{0.25 \times 10^{-24}}{\left(\frac{E}{cm^2}\right)^2} \left[\frac{-1}{\sin^2\theta}\right]_{\theta^{min}}^{\theta^{max}} \tag{36}$$

for a 50 Mev incident proton. In order to get the range of E_s energies indicated, we need

$$\sin^2\theta^{max} = \frac{1}{50} \quad \text{and} \quad \sin^2\theta^{min} = \frac{.0005}{50} .$$

This gives a total cross section of $\sigma = 2 \times 10^{-24}$ cm^2. Using a high-energy-proton flux of 10^4 proton/cm^2-sec and a thermal proton population of 10^4 atoms/cm^3, we get a slow proton product in rate S_p of

$$S_p = \left(10^4 \frac{\text{fast protons}}{\text{cm}^2\text{-sec}}\right)\left(10^4 \frac{\text{H atoms}}{\text{cm}^3}\right)\left(2 \times 10^{-24}\ \text{cm}^2\right)$$

$$S_p = 2 \times 10^{-16} \frac{\text{protons}}{\text{cm}^3\text{-sec}} \text{ of } 0.5 \text{ kev} < E_p < 1 \text{ Mev.}$$

This source strength is considerably less than neutron-decay source strength, and the proton lifetimes will be shorter here too because the protons made are of lower average energy. Therefore, this source produces an even smaller fraction of the observed protons and is not important.

We can ask another question. Is there enough energy in the high-energy protons to supply the low-energy protons by any process? Using a proton lifetime of 10^6 sec and velocity of 5×10^8 cm/sec, we get the energy requirement of the low-energy-proton source of

$$\left(50 \frac{\text{ergs}}{\text{cm}^2\text{-sec}}\right)\left(\frac{1}{5 \times 10^8 \frac{\text{cm}}{\text{sec}}}\right)\left(\frac{1}{10^8\ \text{sec}}\right) = 10^{-13} \frac{\text{ergs}}{\text{cm}^3\text{-sec}} .$$

The energy loss rate E_L of inner-belt high-energy protons is about

$$E_L = \left(50 \frac{\text{Mev}}{\text{protons}}\right)\left(1.6 \times 10^{-6} \frac{\text{erg}}{\text{Mev}}\right)\left(10^4 \frac{\text{protons}}{\text{cm}^2\text{-sec}}\right)\left(\frac{1}{10^{10} \frac{\text{cm}}{\text{sec}}}\right)\left(\frac{1}{10^8\ \text{sec}}\right) = 8 \times 10^{-19} \frac{\text{erg}}{\text{cm}^3\text{-sec}} ,$$

where we have assumed an average lifetime of 10 seconds.

We see that energetically the high-energy protons cannot produce the low-energy protons by any process. The energy in the low-energy protons must come from some other sources that are currently not understood. These low-energy protons are one of the most interesting mysteries of the radiation belt.

ELECTRONS

It seems surprising, but we know a good deal less about the electrons in the inner belt than about those in the outer belt. One reason for this is that the high-energy protons present in the inner belt tend to hide the electrons. The protons are counted with high efficiency by most detectors and penetrate considerable amounts of shielding. Instruments designed to count electrons will usually count the protons too.

There are, however, several experiments that have given some information about the inner belt electrons.

Measurement of the Electron Spectrum

Several particle spectrometers have been flown on pods on Atlas rockets, by Holly, et al. (Reference 59) to altitudes up to 1500 km in the inner belt near the equator. Electrons were identified by the use of magnetic analysis. The differential energy spectrum of the electrons measured here is shown in Figure 15.

The inner belt electron spectrum has also been measured recently by a 10-channel magnetic spectrometer flown on Discoverer satellites at about 400 km (Reference 60). In the Atlantic Ocean off Brazil, a region of high count rate was observed; this region connects to the inner belt (Reference 61). Vernov found that this region had a high content of protons by comparing the count rates of a GM counter and a scintillation counter. The spectrometer on Discoverer satellites 29 and 31 had a blank channel to count protons which were considered a background for this experiment and subtracted from the data. The electron spectrum measured in the South Atlantic by a Discoverer is shown in Figure 15.

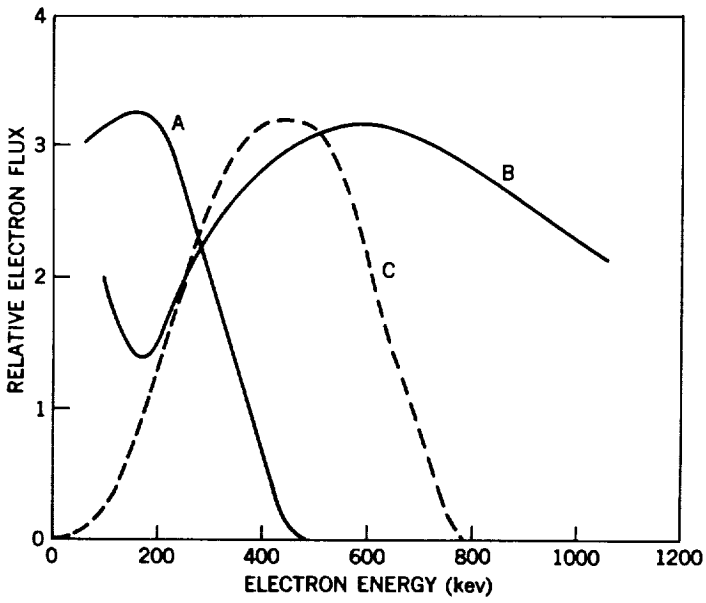

Figure 15—Electron-energy spectra in the inner belt: Curve A measured by Holly, Allen, and Johnson; curve B measured by Bame, Conner, et al. (Reference 55); curve C is a calculated spectrum based on a neutron decay source.

The count rate here is due to inner belt electrons that have come down to low altitudes at this location because the magnetic field is weak. This spectrum extends to higher energies and is flatter than the Atlas pod spectrum. The difference in these two spectra is not understood; they were not measured at the same time or place, so a direct comparison is really not possible. The Discover spectrometer did see other types of electron energy spectra in other places, but never any type resembling the spectrum of

Reference 59. In the South Atlantic the only spectrum seen is that shown in Figure 15.

The energy spectrum expected (References 62, 63, and 64) in the inner belt from neutron β-decay electrons is also shown in Figure 15. Electrons are lost from the inner belt by coulomb collisions which change the pitch angle and cause the particles to diffuse out of the loss cone. The energy dependence of the electrons lifetime τ as calculated for scattering is (Reference 65)

$$\tau \propto v p^2 ,$$

where p = electron momentum and v = electron velocity. The shape of the equilibrium electron spectrum expected from neutron β-decay is simply the shape of the β-decay spectrum (see Figure 2) weighted by the particles' lifetimes which change with energy as given above. This calculated spectrum lies between the two experimental spectra.

The situation here is not clear. It appears experimentally that the inner belt electron spectrum may vary with space or time. But the observed spectra do not seem to agree very well with the spectrum calculated from neutron decay. It appears that sometimes there are electrons of $E > 1.2$ Mev in the inner belt. These cannot be directly made by neutron decay. Some acceleration process must act to produce these high-energy electrons. It would seem that neutron decay electrons could be accelerated most easily because they start with relatively high energies to begin with. We must wait for more experimental information to make any kind of quantitative comparison with calculations based on neutron decay.

The Electron Flux

There have been several measurements which give the electron flux in the radiation belts. None of these are for the central regions of the inner belt, but we can interpolate what measurements are available to give reasonable estimates in the inner belt.

There are three measurements of the electron flux at about 1000 km altitude. O'Brien, et al. (Reference 66) have measured the flux of electrons of $E_e > 40$ kev at 1000 km on the Injun satellite by using magnetic spectrometers. The flux thus determined was about 10^5 to 10^6 electrons/cm^2-sec-ster so, because $\Delta\Omega \approx 1$ ster at these altitudes, the omnidirectional flux is $\Phi_e \approx 10^5$ to 10^6 electrons/cm^2-ster. These measurements were for $L > 2$ so they are not really inner-zone electron fluxes. The electron flux of $E_e > 30$ kev measured by Holly, et al. (Reference 59) at 980 km was about 7×10^5 electrons/cm^2-sec. This was at 15° N latitude and is truly an inner belt flux. Cladis, et al. (Reference 67) measured an electron flux for $E > 50$ kev of 4×10^6 electrons/cm^2-sec at $L \sim 2.4$ using a magnetic spectrometer; these measurements give an electron flux at 100 km of the order of 10^6 electrons/cm^2-sec of $E > 40$ kev.

Equipment on the Explorer XII (1961υ) satellite has measured the electron flux in the outer belt. O'Brien, et al. (Reference 68) report fluxes going up to 10^8 electrons/cm^2-sec of $E > 40$ kev, but a more typical

flux (Reference 69) is about 10^7 electrons/cm^2-sec. The electron flux is quite constant from about 50,000 km into about 10,000 km.

From this data we can guess that the electron flux in the center of the inner belt is about 10^7 electrons/cm^2-sec, possibly going as high as 10^8 electrons/cm^2-sec.

One early measurement seemed to give information about the inner-belt electron flux, but this now appears incorrect.

The Explorer IV satellite carried four detectors that detected particles of different ranges. The particles that penetrated 1 gm/cm^2 or more of shielding were identified as being high-energy protons (Reference 13).

One detector on Explorer IV, the energy scintillator, counted particles that penetrated 1.0 mg/cm^2 of shielding. A large flux, up to 10 ergs/cm^2-sec-ster or more, was measured by this detector. A tentative analysis of this experiment (Reference 13) suggested it was due to electrons that would just penetrate the 1 mg/cm^2 foil of about 20 kev. This model was proposed by analogy with early ideas about the composition of the outer belt. Assuming the particles were 20 kev, it took about 2×10^9 electrons/cm^2-sec-ster to give the observed energy flux.

But it now appears that this interpretation was not correct. Recently, on the Injun satellite, an energy flux of up to 100 ergs/cm^2-sec of heavy ions was measured (Reference 58). These were very probably protons and they were in the energy range of 0.5 kev to 1 Mev. Many of these particles would be counted by the Explorer IV energy scintillator. It, therefore, seems likely that this Explorer IV counter was counting low-energy protons and not electrons.

The inner-belt electron flux expected from neutron decay is of the same order of magnitude as the observed flux. Wentworth, et al. (Reference 65) have calculated the electron lifetime for coulomb scattering by solving the Fokker-Planck equation. For an atmospheric He density at 2000 km of $\bar{\rho} = 10^5$ atoms/cm^3 they get a lifetime for a 300 kev electron of $\tau_e = 1.5 \times 10^8$ sec. Using this lifetime and the source strength (Reference 26) of 3×10^{-12} electrons/cm^3-sec, we get an equilibrium electron flux of

$$\Phi_e = \left(3 \times 10^{12} \frac{\text{electrons}}{\text{cm}^3\text{-sec}}\right)\left(3 \times 10^{10} \frac{\text{cm}}{\text{sec}}\right)\left(1.5 \times 10^8 \text{ sec}\right) \approx 10^7 \frac{\text{electrons}}{\text{cm}^2\text{-sec}} \quad .$$

In comparing the observations of electrons with calculations based on the neutron-decay theory, we find that the calculated and observed fluxes are quite similar but that the spectra are not in as obvious agreement. It is quite certain that neutron-decay electrons produce a large fraction of the trapped electrons. It is also quite certain that acceleration processes also operate to generate the high-energy electrons.

OTHER PARTICLES

If the sun were the source of particles in the inner radiation belt we would expect to find not only protons but other heavier particles such as deuterons, tritons, and He^3 and He^4 nuclei. The sun contains about 15 percent He nuclei (Reference 70) and solar cosmic rays contain about 5 percent He nuclei (Reference 71). The lifetime of a He^4 nuclei in the inner belt would be about five times less than that of a proton of the same energy because the rate of slowing down is faster for $Z = 2$. On this basis, we would expect about 1 percent He^4 in the inner belt. But experimentally not one $Z = 2$ track has been found in nuclear emulsion. The total number of particles measured in three experiments is given in Table 5.

Table 5

Measurements on Trapped Heavy Particles.

Experiment	No. of Protons	No. of Deuterons	No. of Tritons	No. of Alphas
Freden and White May 1959 (Reference 33)	243	0	3	0
Armstrong, et al. July 1959 (Reference 34)	477	5	0	0
Heckman and Armstrong October 1960 (Reference 36)	301	0	0	0
Total	1021	5	3	0

An upper limit of the α flux is 0.1 ± 0.05 percent of the proton flux in the energy interval 125 to 185 Mev (Reference 36). This quite clearly shows that the sun contributes few, if any, of the heavy particles in the inner belt.

A few deuterons and tritons (roughly 1/2 percent each) were found in the emulsion experiments as is shown in Table 5. These particle fluxes can be explained (Reference 33) as being the result of nuclear collisions of trapped protons with O and N nuclei in the very thin atmosphere present at radiation belt altitudes. No heavy particles have been observed in the inner belt that cannot be understood by the neutron-decay source.

CONCLUSIONS

From the foregoing discussion we can draw the following conclusions about the inner radiation belt:

The high-energy protons (E_p > 30 Mev) result from galactic cosmic-ray production of neutrons in the earth's atmosphere and the subsequent escape and decay of these neutrons. Both the energy spectrum and the intensity of the trapped protons are completely consistent with this interpretation. The time variations observed in this proton population are understood well in terms of solar-cycle variations in the exosphere density and of cosmic-ray flux.

The spatial distribution of these protons also seems reasonable on the basis of neutron decay injection. Protons are lost from the belt by slowing down. Increasing density of air limits the lower edge of the belt, and the changes in altitude of the lower edge with longitude are due to changes in the strength of the earth's field. The belt's outer edge is probably controlled by hydromagnetic waves which change the protons' magnetic moment and scatter them into the atmosphere. As far as we know now, these protons are made from neutrons and from no other sources.

Medium-energy protons (5 Mev < E_p < 30 Mev) seem to be made from neutron decay by two different processes: In the inner part of the inner belt, for L < 1.6 where the spectrum is rather flat, the protons are quite certainly due to neutrons made by galactic cosmic-ray protons. Out farther, for L > 1.7, the steeper spectrum and larger fluxes are quite certainly due to the decay of neutrons made by solar protons striking the polar regions at the times of some solar flares.

The newly discovered low-energy protons (0.5 kev < E_p < 1 Mev) might either be made by some quite new and different and not understood source, or they might be accelerated from a lower-energy source (such as slow neutron-decay protons or knock-on protons) to the observed energies. One thing is quite certain: neutron-decay protons do not supply a large fraction of the total energy in these protons directly.

The origin of the trapped electrons in the inner belt is not as well established because there have been few experiments to study their characteristics. The flux is not known to an order of magnitude and the spectrum is also uncertain, but it would appear that the energy spectrum goes up past 1 Mev and the flux is of the order 10^7 electrons/cm^2-sec. From neutrons we would expect a flux of about 10^7 and a spectrum ending at 780 kev. The high-energy electrons (E > 780 kev) are not produced by neutron decay directly, but it would seem that some acceleration processes operating on neutron-decay electrons to increase their energy is the most probable source mechanism for these electrons. If we use an accelerating process operating on low-energy electrons to generate the observed electrons, the requirements on the accelerating process are considerably increased.

Our conclusion is that the inner-belt protons of E > 5 Mev are produced by neutron decay from galactic and solar protons, but the E < 1 Mev protons are of different and unknown origin. The inner-belt electrons are probably made by a combination of neutron decay and some uncertain acceleration process.

REFERENCES

1. Van Allen, J. A., Ludwig, G. H., et al., "Observation of High Intensity Radiation by Satellites 1958 Alpha and Gamma," *Jet Propulsion* 28(9):588-592, September 1958.

2. Van Allen, J. A., "First Public Lecture on the Discovery of the Geomagnetically-Trapped Radiation," State Univ. of Iowa, SUI 60-13, 1960.

3. Störmer, C., "The Polar Aurora," Oxford: Clarendon Press, 1955.

4. Van Allen, J. A., "Dynamics, Composition and Origin of the Geomagnetically-Trapped Corpuscular Radiation," State Univ. of Iowa, SUI 61-19, August 1961.

5. Chapman, S., and Bartels, J., "Geomagnetism," Oxford: Clarendon Press, 1940.

6. Post, R. F., "Controlled Fusion Research – An Application of the Physics of High Temperature Plasmas," *Rev. Mod. Phys.* 28(3):338-362, July 1956.

7. Christofilos, N. C., "The Argus Experiment," *J. Geophys. Res.* 64(8):869-875, August 1959.

8. Vernov, S. N., and Chudakov, A. E., "Terrestrial Corpuscular Radiation and Cosmic Rays," in: *Space Research: Proc. 1st Internat. Space Sci. Sympos., Nice, January 1960,* Amsterdam: North-Holland Publ. Co., 1960, pp. 751-796.

9. Krassovsky, V. I., Shklovsky, I. S., et al., "On Fast Corpuscles of the Upper Atmosphere," in: *"Proc. Internat. Conf. of Cosmic Radiation, Moscow, July 1959,* Moscow, Academie Nauk, 1960, Vol. 3, pp. 59-63.

10. Van Allen, J. A., McIlwain, C. E., and Ludwig, G. H., "Radiation Observations with Satellite 1958ϵ," *J. Geophys. Res.* 64(3):271-286, March 1959.

11. Van Allen, J. A., McIlwain, C. E., and Ludwig, G. H., "Satellite Observations of Electrons Artificially Injected into the Geomagnetic Field," *J. Geophys. Res.* 64(8):877-891, August 1959.

12. Van Allen, J. A., and Frank, L. A., "Radiation around the Earth to a Radial Distance of 107,400 km," *Nature* 183(4659):430-434, February 14, 1959; Also State Univ. of Iowa, SUI 59-2, 1959.

13. Van Allen, J. A., and Frank, L. A., "Radiation Measurements to 658,300 km with Pioneer IV," *Nature* 184(4682):219-224, July 25, 1959; Also State Univ. of Iowa, SUI 59-18, August 1959.

14. Alfvén, H., "Cosmical Electrodynamics," Oxford, Clarendon Press, 1950.

15. Spitzer, L., Jr., "Physics of Fully Ionized Gases," New York: Interscience Publ., 1956.

16. Christofilos, N. C., "Trapping and Lifetime of Charged Particles in the Geomagnetic Field," Univ. Calif. Radiation Lab. Rept. UCRL-5407, November 28, 1958.

17. Gold, T., "Plasma and Magnetic Fields in the Solar System," *J. Geophys. Res.* 64(11):1665-1674, November 1959.

18. Herlofson, N., "Diffusion of Particles in the Earth's Radiation Belts," *Phys. Rev. Letters* 5(9):414-416, November 1, 1960.

19. Rosenbluth, M. N., and Longmire, C. L., "Stability of Plasmas Confined by Magnetic Fields," *Ann. of Physics* 1(2):120-140, May 1957.

20. Northrop, T. G., and Teller, E., "Stability of the Adiabatic Motion of Charged Particles in the Earth's Field," *Phys. Rev.* 117(1):215-225, January 1, 1960.

21. Gall, R., and Lifshitz, J., "Temporary Capture of Cosmic Ray Particles and their Contribution to the High Intensity Belts," *Nuovo Cimento* 15(2):233-245, January 16, 1960.

22. Bridge, H. S., Dilworth, C., et al., "Direct Observations of the Interplanetary Plasma," in: *Proc. Internat. Conf. on Cosmic Rays and the Earth Storm, Kyoto, September 1961. II. Main Sessions*, Tokyo: Physical Society of Japan, 1962, pp. 553-560.

23. Chang, C. C., "Outer Van Allen Belts and Neutral Points on Interface Between Solar Wind and Geomagnetic Field," *Nature* 194(4827):424-426, May 5, 1962.

24. Axford, W. I., and Hines, C. O., "A Unifying Theory of High-Latitude Geophysical Phenomena and Geomagnetic Storms," *Can. J. Phys.* 39(10):1433-1464, October 1961.

25. Hess, W. N., and Starnes, A. J., "Measurement of the Neutron Flux in Space," *Phys. Rev. Letters* 5(2):48-50, July 15, 1960.

26. Hess, W. N., Canfield, E. H., and Lingenfelter, R. E., "Cosmic-Ray Neutron Demography," *J. Geophys. Res.* 66(3):665-677, March 1961.

27. Hess, W. N., Patterson, H. W., et al., "Cosmic-Ray Neutron Energy Spectrum," *Phys. Rev.* 116(2):445-457, October 15, 1959.

28. Stuart, G. W., "Satellite-Measured Radiation," *Phys. Rev. Letters* 2(10):417-418, May 15, 1959.

29. Fite, W. L., Stebbings, R. F., et al., "Ionization and Charge Transfer in Proton-Hydrogen Atom Collisions," *Phys. Rev.* 119(2):663-668, July 15, 1960.

30. Orear, J., Rosenfeld, A. H., and Schluter, R. A. (Comp.), "Nuclear Physics; A Course Given by Enrico Fermi at the University of Chicago," Rev. Ed., Chicago: University of Chicago Press, 1950.

31. Freden, S. C., and White, R. S., "Protons in the Earth's Magnetic Field," *Phys. Rev. Letters* 3(1):9-11, July 1, 1959.

32. Freden, S. C., and White, R. S., "Trapped Proton and Cosmic-Ray Albedo Neutron Fluxes," *J. Geophys. Res.* 67(1):25-29, January 1962.

33. Freden, S. C., and White, R. S., "Particle Fluxes in the Inner Radiation Belt," *J. Geophys. Res.* 65(5):1377-1383, May 1960.

34. Armstrong, A. H., Harrison, F. B., et al., "Charged Particles in the Inner Van Allen Radiation Belt," *J. Geophys. Res.* 66(2):351-357, February 1961.

35. Naugle, J. E., and Kniffen, D. A., "Flux and Energy Spectra of the Protons in the Inner Van Allen Belt," *Phys. Rev. Letters* 7(1):3-6, July 1961.

36. Heckman, H. H., and Armstrong, A. H., "Energy Spectrum of Geomagnetically Trapped Protons," *J. Geophys. Res.* 67(4):1255-1262, April 1962.

37. Singer, S. F., "Trapped Albedo Theory of the Radiation Belt," *Phys. Rev. Letters* 1(5):181-183, September 1, 1958.

38. Singer, S. F., "Latitude and Altitude Distribution of Geomagnetically Trapped Protons," *Phys. Rev. Letters* 5(7):300-303, October 1, 1960.

39. Lenchek, A. M., and Singer, S. F., "Geomagnetically Trapped Protons from Cosmic-Ray Albedo Neutrons," *J. Geophys. Res.* 67(4):1263-1288, April 1962.

40. Hess, W. N., "Van Allen Belt Protons from Cosmic-Ray Neutron Leakage," *Phys. Rev. Letters* 3(1):11-13, July 1, 1959.

41. Harris, I., and Priester, W., "Theoretical Models for the Solar-Cycle Variation of the Upper Atmosphere," NASA Technical Note D-1444, August 1962.

42. Ray, E. C., "On the Theory of Protons Trapped in the Earth's Magnetic Field," *J. Geophys. Res.* 65(4):1125-1134, April 1960.

43. Yoshida, S., Ludwig, G. H., and Van Allen, J. A., "Distribution of Trapped Radiation," *J. Geophys. Res.* 65(3):807-813, March 1960.

44. Fan, C. Y., Meyer, P., and Simpson, J. A., "Dynamics and Structure of the Outer Radiation Belt," *J. Geophys. Res.* 66(9):2607-2640, September 1961.

45. Welch, J. A., and Whitaker, W. A., "Theory of Geomagnetically Trapped Electrons from an Artificial Source," *J. Geophys. Res.* 64(8):909-922, August 1959.

46. Dragt, A. J., "Effect of Hydromagnetic Waves on the Lifetime of Van Allen Radiation Protons," *J. Geophys. Res.* 66(6):1641-1649, June 1961.

47. Wentzel, D. G., "Hydromagnetic Waves and the Trapped Radiation. Part 2. Displacements of the Mirror Points," *J. Geophys. Res.* 66(2):363-369, February 1961.

48. Parker, E. N., "Effect of Hydromagnetic Waves in a Dipole Field on the Longitudinal Invariant," *J. Geophys. Res.* 66(3):693-708, March 1961.

49. Hamlin, D. A., Karplus, R., et al., "Mirror and Azimuthal Drift Frequencies for Geometrically Trapped Particles," *J. Geophys Res.* 66(1):1-4, January 1961.

50. Fermi, E., "On the Origin of Cosmic Radiation," *Phys. Rev.* 75(8):1169-1174, April 15, 1949.

51. McIlwain, C. E., "Coordinates for Mapping the Distribution of Magnetically Trapped Particles," *J. Geophys. Res.* 66(11):3681-3691, November 1961.

52. Rothwell, P., and McIlwain, C. E., "Magnetic Storms and the Van Allen Radiation Belts—Observations from Satellite 1958ϵ (Explorer IV)," *J. Geophys. Res.* 65(3):799-806, March 1960.

53. Armstrong, A. H., and Heckman, H. H., "Flux and Spectrum of Charged Particles in the Lower Van Allen Belt," *Bull. Amer. Phys. Soc.* 6(4):361, June 22, 1961 (Abstract).

54. Pizzella, G., McIlwain, C. E., and Van Allen, J. A., "Time Variations of Intensity in the Earth's Inner Radiation Zone, October 1959 through December 1960," *J. Geophys. Res.* 67(4):1235-1254, April 1962.

55. Bame, S. J., Conner, J. P., et al., "Protons in the Outer Van Allen Belt," *J. Geophys. Res.* 68(1):55-63, January 1963.

56. Lenchek, A. M., "On the Anomalous Component of Low-Energy Geomagnetically Trapped Protons," *J. Geophys. Res.* 67(6):2145-2157, June 1962.

57. Webber, W. R., "Time Variations of Low Energy Cosmic Rays during the Recent Solar Cycle," in: *Progress in Elementary Particle and Cosmic Ray Physics*, ed. by J. G. Wilson and S. A. Wouthuysen, Amsterdam: North-Holland Publ. Co., Vol. 6, 1962 (In Press).

58. Freeman, J. W., "Detection of an Intense Flux of Low-Energy Protons or Ions Trapped in the Inner Radiation Zone," *J. Geophys. Res.* 67(3):921-928, March 1962.

59. Holly, F. E., Allen, L., and Johnson, R. G., "Radiation Measurements to 1500 Kilometers Altitude at Equatorial Latitudes," *J. Geophys. Res.* 66(6):1627-1639, June 1961.

60. Mann, L. G., Bloom, S. D., and West, H. I., Jr., "The Electron Spectrum from 80 to 1258 Kev Observed on Discoverer Satellites 29 and 31," Paper presented at the 3rd Internat. Space Sci. Sympos., Washington, May 1962.

61. Vernov, S. N., Savenko, I. A., et al., "Discovery of the Internal Radiation Belt at a Height of 320 km in the Region of the South Atlantic Magnetic Anomaly," *Doklady Akademii Nauk SSSR* 140(5):1041-1044, October 11, 1961. Translation in *Soviet Phys. — Doklady* 6(10):893-896, April 1962.

62. Kellogg, P. J., "Electrons of the Van Allen Radiation," *J. Geophys. Res.* 65(9):2705-2713, September 1960.

63. Lenchek, A. M., Singer, S. F., and Wentworth, R. C., "Geomagnetically Trapped Electrons from Cosmic Ray Albedo Neutrons," *J. Geophys. Res.* 66(12):4027-4046, December 1961.

64. Hess, W. N., and Poirier, J. A., "Energy Spectrum of Electrons in the Outer Radiation Belt," *J. Geophys. Res.* 67(5):1699-1709, May 1962.

65. Wentworth, R. C., MacDonald, W. W., and Singer, S. F., "Lifetimes of Trapped Radiation Belt Particles Determined by Coulomb Scattering," *Physics of Fluids* 2(5):499-509, September-October 1959.

66. O'Brien, B. J., Langhlin, C. D., et al., "Measurements of the Intensity and Spectrum of Electrons at 1000-Kilometer Altitude and High Latitudes," *J. Geophys. Res.* 67(4):1209-1226, April 1962.

67. Cladis, J. B., Chase, L. F., et al., "Energy Spectrum and Angular Distributions of Electrons Trapped in the Geomagnetic Field," *J. Geophys. Res.* 66(8):2297-2312, August 1961.

68. O'Brien, B. J., Van Allen, J. A., et al., "Absolute Electron Intensities in the Heart of the Earth's Outer Radiation Zone," *J. Geophys. Res.* 67(1):397-403, January 1962.

69. Rosser, W. G. V., O'Brien, B. J., et al., "Electrons in the Earth's Outer Radiation Zone," Paper presented at 43rd Annual Meeting Amer. Geophys. Union, Washington, April 1962.

70. Aller, L. H., "Astrophysics; the Atmospheres of the Sun and Stars," New York: Ronald Press, 1953.

71. Biswas, S., Fichtel, C. E., and Guss, D. E., "A Study of the Hydrogen, Helium and Heavy Nuclei in the November 12, 1960 Solar Cosmic Ray Event," *Phys. Rev.* 128(6):2756-2771, December 1962.

NASA-Langley, 1963 G-279